Journal of the Geological Society

Ediacaran Gaskiers Glaciation of Newfoundland reconsidered

G. J. Retallack

Journal of the Geological Society 2013, v.170; p19-36.
doi: 10.1144/jgs2012-060

Notes

Journal of the Geological Society, London, Vol. **170**, 2013, pp. 19–36. doi: 10.1144/jgs2012-060.

Ediacaran Gaskiers Glaciation of Newfoundland reconsidered

G. J. RETALLACK*

Department of Geological Sciences, University of Oregon, Eugene, OR 97403, USA

**Corresponding author (e-mail: gregr@uoregon.edu)*

Abstract: Newly discovered palaeosols in the Gaskiers Formation of Newfoundland provide a new perspective on its palaeoenvironment, and are evidence that it was not a deep submarine tillite, nor an anoxic deep-sea floor, nor a 'cap carbonate' from extreme geochemical perturbation of the global ocean. Discovery of oxidized palaeosols and re-evaluation of sedimentary facies and stratigraphic relationships now suggest reinterpretation as a coastal plain with glacial moraines in the forearc basin of a continental volcanic arc, like modern Japan. Ediacaran palaeosols of the Gaskiers Formation lack large root traces, but show soil profile differentiation (clay enrichment and depletion of alkali and alkaline earth elements at the expense of feldspar and rock fragments) and diagnostic soil structures (blocky peds, argillans, sepic plasmic fabric). These palaeosols are evidence of a humid temperate climate and marked marine regression accompanying the Gaskiers Glaciation of the early Ediacaran (580 Ma). Geochemical weathering trends in the palaeosols, especially phosphorus depletion, are characteristic of biologically active soils. Ediacaran microbial earth ecoystems may have been responsible for filamentous disruption of bedding in the palaeosols.

The Gaskiers Formation of eastern Newfoundland (Fig. 1) has been considered evidence of deep-sea anoxia immediately preceding deep oceanic oxidation (Canfield *et al*. 2007), which in turn paved the way for evolutionary radiation of Ediacaran fossils (Fig. 2). Diamictites of the Gaskiers Formation have been considered evidence for Ediacaran (581–580 Ma; Bowring *et al*. 2003) marine ice shelves (Anderson & King 1981; Eyles & Eyles 1989; Carto & Eyles 2011). Gaskiers Glaciation postdated the hypothetical Cryogenian 'Snowball Earth' freezings of the world ocean (Hoffman *et al*. 1998; Hoffman & Schrag 2002; Hoffman & Li 2009), but like these extreme geochemical perturbations the Gaskiers Formation may have had an 'unusual cap carbonate' with anomalous stable isotopic values for oxygen and carbon (Myrow & Kaufman 1999). These various interpretations are here re-evaluated from the perspective of newly discovered palaeosols in the Gaskiers Formation, which provide new grounds for understanding the palaeogeographical and palaeoclimatic setting of the Gaskiers Glaciation.

This paper is mainly a contribution to the vexing problem of recognizing palaeosols in pre-Devonian sedimentary rocks, predating the evolution of roots and other modern soil biota (Retallack 2011*a*, *b*, 2012*a*, *b*). Palaeosols in Precambrian sedimentary sequences have been widely overlooked because they lack root traces (Retallack 1997), and other diagnostic features of palaeosols such as soil horizons and soil structures can be subtle. The sharp top and gradational changes of soil horizons, for example, can be misinterpreted for graded beds (Retallack 2012*a*). The hackly structure of soil clods (peds defined by cutans) can be obscured by metamorphic cleavage or modern weathering (Retallack 2012*b*). Chemical differentiation of palaeosols by hydrolysis, and other diagnostic chemical proxies, must thus assume a prominent role in the recognition and interpretation of Precambrian palaeosols (Retallack 2012*a*, *b*). Precambrian palaeosols have been widely recognized at geological unconformities (Rye & Holland 1998), but are seldom considered in evaluation of Precambrian sedimentary rocks.

This study was stimulated by discrepancies between three published geochemical proxies (Canfield *et al*. 2007) and deep marine palaeoenvironments inferred for the Conception and St. Johns Groups of Newfoundland (Gardiner & Hiscott 1988; Eyles & Eyles 1989; Wood *et al*. 2003; Ichaso *et al*. 2007). First, high C/S ratios (>2.8) are evidence of freshwater, not marine, palaeoenvironments (Berner & Raiswell 1984; Raiswell & Berner 1986). Second, low ratios (<0.2) of highly reactive iron (Fe_{HR}, mainly in pyrite or hematite) and total iron (including iron still within silicates, Fe_{TOT}) are evidence of soils, not marine or lacustrine sediments (Ku *et al*. 2008). Third, negative values for the isotopic composition of sulphur in pyrite ($\delta^{34}S$ v. CDT‰) are evidence of sulphate-reducing bacteria common in euxinic oceans as well as intertidal mudflats (Altschuler *et al*. 1983; Canfield & Farquhar 2009). All three lines of geochemical proxy data from Newfoundland Ediacaran rocks (in supplementary data of Canfield *et al*. 2007) reveal a mix of marine and non-marine palaeoenvironments (Figs 2 and 3), including local sulphate reduction that was not in black shales, and therefore was more like intertidal than euxinic pyritization (Berner & Raiswell 1984; Raiswell & Berner 1986). The implication that several horizons in the Gaskiers Formation were fresh in the sense of low salinity or low sulphate, or both, and as highly oxidized as modern soils is difficult to explain by non-analogue Ediacaran ocean chemistry (Canfield *et al*. 2007), because it requires Ediacaran ocean sulphate and organic carbon concentrations like those of modern Swiss lakes (Canfield *et al*. 2010). This could not have been typical of the Ediacaran ocean because modern marine C/S ratios were found at other stratigraphic levels (Fig. 2), and it is more likely that facies changed on million year time scales rather than ocean composition. There were thus already grounds to doubt deep marine palaeoenvironments for the Gaskiers, and associated formations.

Materials and methods

Exposures of the Gaskiers Formation examined for this work were in sea cliffs 2 km west of St. Marys (Fig. 4b; 46.91933°N, 53.59828°E), and across the road from the Peter and Paul Church in Harbour Main (Fig. 4a; 47.44018°N, 53.15696°E), Newfoundland. Oriented rock specimens for analysis are from stratigraphic sections measured using level and tape. Petrographic thin sections were point counted for grain size fractions and mineral content (Tables 1 and 2) with error of ±2% (Murphy 1983). Specimens were also analysed for major elements by X-ray fluorescence (XRF), for organic carbon using the Walkley–Black titration, and for ferrous iron using Pratt

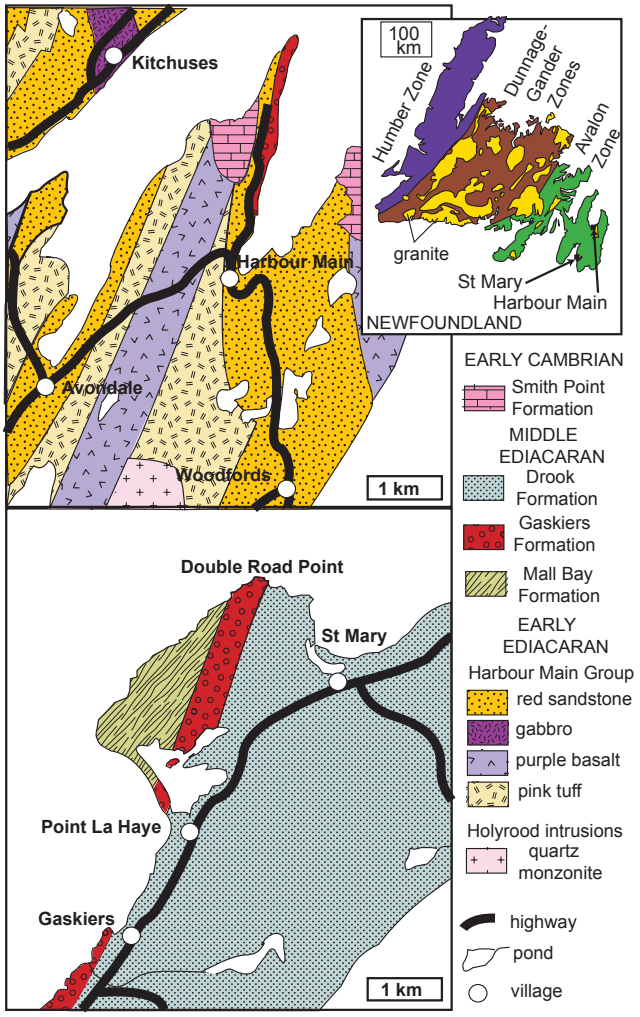

Fig. 1. Geological maps of Newfoundland terranes (inset), and two localities of the Gaskiers Formation examined for this study.

titration by ALS Chemex of Vancouver, BC (Table 3). Sand crystal abundance was estimated in the field using a comparative card of Terry & Chilingar (1955).

The characteristic chemical reaction of soil formation is hydrolysis, incongruent dissolution of weatherable minerals such as feldspar and biotite in carbonic acid from soil carbon dioxide to produce clay and cations in solution (Retallack 1997). The most common of these cations are Ca^{2+}, Mg^{2+}, Na^{+}, and K^{+}, whose abundance at different levels within a palaeosol can be determined by major element chemical analysis. As recommended by Brimhall *et al*. (1992), the mass transfer of elements in a soil at a given horizon ($\tau_{w,j}$ in moles) was calculated from the bulk density of the soil (ρ_w in g cm^{-3}) and parent material (ρ_p in g cm^{-3}) and from the chemical concentration of the element in soils ($C_{j,w}$ in wt%) and parent material ($C_{p,w}$ in wt%). Changes in volume of soil during weathering were called strain by Brimhall *et al*. (1992), and are estimated from an immobile element in soil (such as Ti used here) compared with parent material ($\varepsilon_{i,w}$ as a fraction). This strain is restricted to the metre or so thicknesses of a single palaeosol profile, and is not affected by burial compaction acting over kilometres. The relevant equations (1) and (2) are the basis for calculating divergence from parent material composition. Subscripts in these equations are for immobile event (i) and chosen element (j) in parent material (p) and soil (w):

$$\tau_{j,w} = \left(\frac{\rho_w \cdot C_{j,w}}{\rho_p \cdot C_{j,p}} \right) (\varepsilon_{i,w} + 1) - 1 \quad (1)$$

$$\varepsilon_{i,w} = \left(\frac{\rho_p \cdot C_{j,p}}{\rho_w \cdot C_{j,w}} \right) - 1. \quad (2)$$

Also calculated was chemical index of alteration (CAI of Nesbitt & Young 1982), now widely applied to Neoproterozoic sedimentary rocks (Rieu *et al*. 2007; Passchier & Erukanure 2010; Bahlburg & Dobrzinksi 2011; Gonzàlez-Àlvarez & Kerrich 2012). Chemical index of alteration (I in mol mol^{-1}) is calculated from molar proportions (m) of alumina, lime, potash and soda according to equation (3) below. The lime is non-carbonate lime, but no correction for carbonates was made because they were rare (one sample with >5% $CaCO_3$ was excluded; Table 3).

$$I = \left[\frac{100 \cdot (m\mathrm{Al_2O_3})}{(m\mathrm{Al_2O_3} + m\mathrm{CaO} + m\mathrm{Na_2O} + m\mathrm{K_2O})} \right] \quad (3)$$

Sedimentological observations

The following new observations and summary of previously published observations on the Gaskiers Formation are offered without interpretation beyond consideration that these are indeed original sedimentary features, rather than artefacts of structural deformation, hydrothermal alteration or metamorphism.

Stratigraphic relationships

To the south near St. Mary (Fig. 1) the Gaskiers Formation is folded with the underlying Mall Bay Formation and overlying Drook Formation (King 1988; Eyles & Eyles 1989). To the north near Harbour Main, a thin (22 m) sequence of Gaskiers Formation lies directly on Harbour Main Volcanic basement, and is overlain by Drook Formation (Myrow & Kaufman 1999). Neither Gaskiers nor Mall Bay Formation crops out to the east of the Conception Bay Anticlinorium, which was a basement ridge of Harbour Main Volcanics, but there are thin red diamictites at comparable stratigraphic levels in the northeastern Avalon Peninsula (in Bauline Line and Torbay Members of the Drook Formation of Fig. 5c; King 1988).

Asymmetric ripple marks and sole marks in the lower Mall Bay Formation have been used to infer palaeocurrents toward the SW, but in the upper Mall Bay Formation these head easterly, and in the lower Drook Formation NE (Gardiner & Hiscott 1988). Such SW–NE basin axial palaeocurrents are evidence that the Gaskiers Formation accumulated in a basin between an uplifted ridge of Harbour Main volcanoes that were still active (O'Brien *et al*. 2001) to the east, and a terrestrial volcanic arc to the west, including the Marystown Volcanics (Rabu *et al*. 1993; McNamara *et al*. 2001; Ichaso *et al*. 2007). The Marystown and Harbour Main Volcanics were a mid-latitude (34° ± 8°S) part of the peri-Gondwanan microcontinent of Avalonia (Evans & Raub 2011; Pisarevsky *et al*. 2012; Thompson *et al*. 2012).

Sediment accumulation rates

The Gaskiers Formation is thick (250–300 m) within a very thick (7595 m) sequence of Ediacaran sedimentary rocks in Newfoundland (Fig. 2). High-precision (±3 Ma) U/Pb dates from zircons in volcanic tuffs constrain the age of the basal Gaskiers

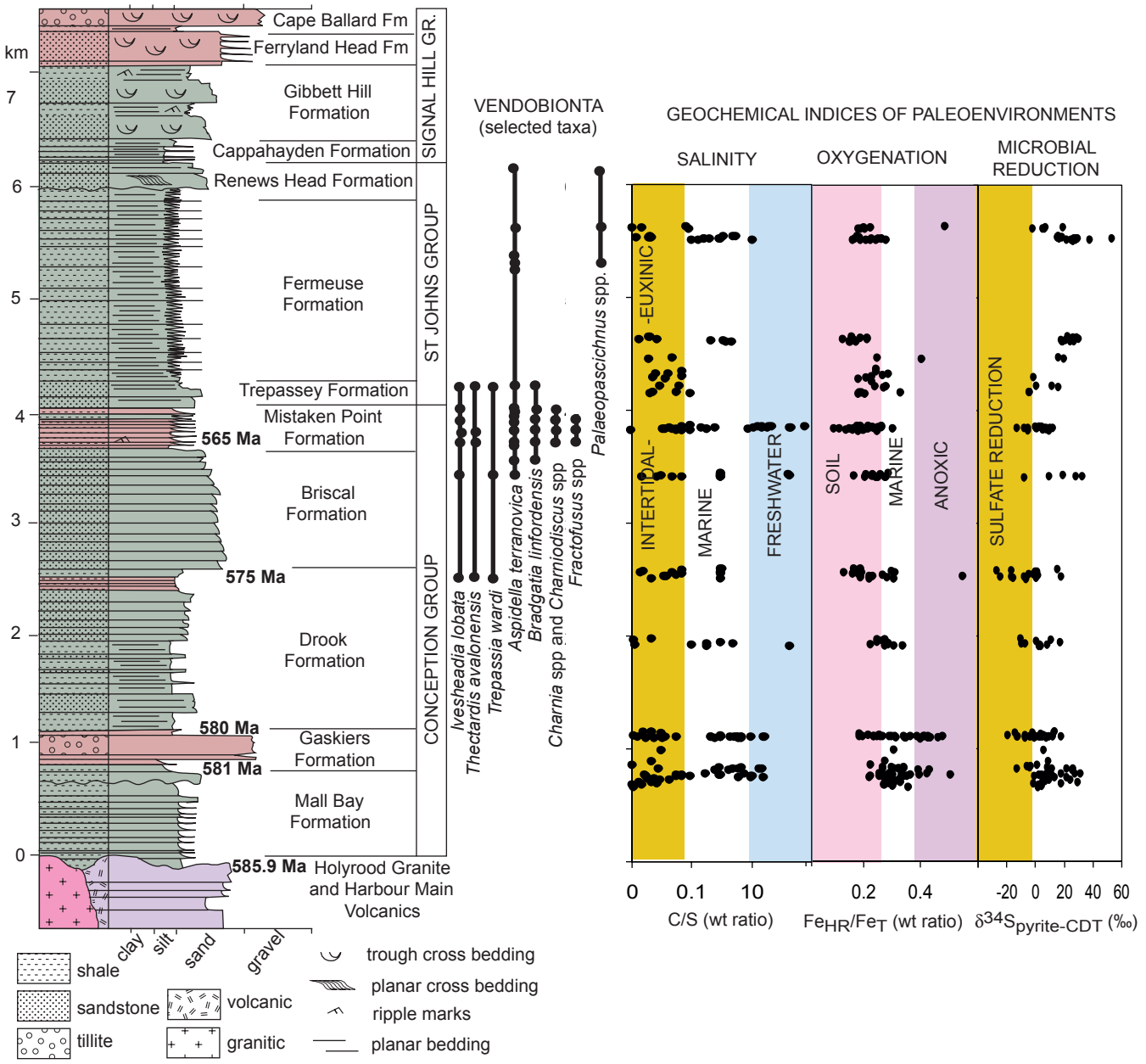

Fig. 2. Ediacaran geological succession of Newfoundland with ranges of selected fossils (after Narbonne *et al*. 2005) and selected palaeoenvironmental proxy data (after Canfield *et al*. 2007) on fields defined for modern environments (in Fig. 3).

Formation (770 m in Fig. 2) to 581 Ma and top Gaskiers Formation (1111 m) to 580 Ma, middle Drook Formation (2550 m) to 575 Ma, and Mistaken Point Formation (4133 m) to 565 Ma (Bowring *et al*. 2003). This is a coherent sequence without stratigraphic break, because regression for age (A in Ma) from thickness (T in m) is highly correlated ($r^2 = 0.97$), and can be described by a linear function:

$$A = 0.0047T + 585.32. \quad (4)$$

The rate of rock accumulation within the Gaskiers Formation was thus 0.30 ± 0.2 mm a^{-1}, and from the basal Gaskiers Formation to the dated level within the Mistaken Point Formation was 0.08 ± 0.006 mm a^{-1}.

Original sedimentary bed thickness (D_s in m) is needed to calculate sediment accumulation rate from current rock thickness (D_p in m) after compaction during burial, and this can be calculated from estimated thickness of overburden (K in km) using a standard compaction formula with physical constants for marine sands (Sheldon & Retallack 2001), as follows:

$$D_s = D_p / \left[-0.51 / \left(\frac{0.49}{e^{0.37K}} - 1 \right) \right]. \quad (5)$$

Such calculations give Gaskiers Formation sediment accumulation rates of 0.57 ± 0.49 m a^{-1} and Gaskiers–Mistaken Point rates of 0.16 ± 0.01 mm a^{-1}. The Gaskiers Formation was deposited unusually rapidly in a region of rapid sedimentation.

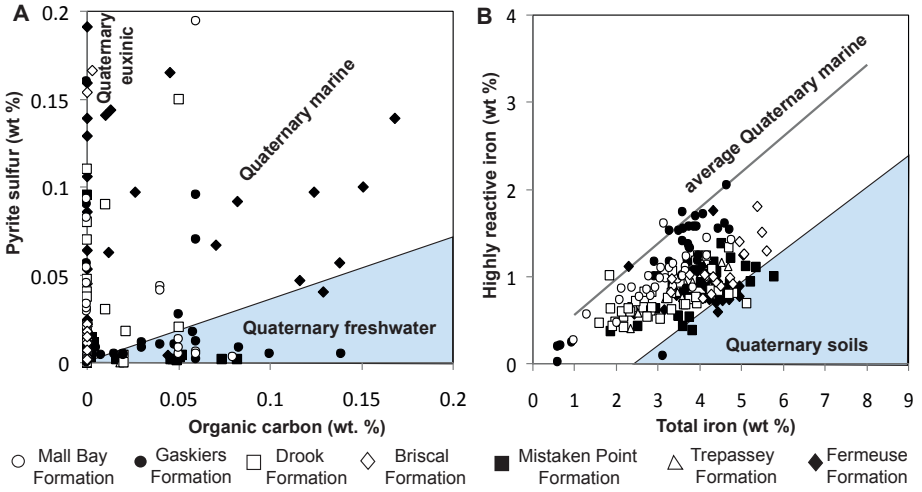

Fig. 3. Analyses from Ediacaran formations of Newfoundland (after Canfield *et al*. 2007) plotted on modern fields for (**a**) C/S ratios (Berner & Raiswell 1984; Raiswell & Berner 1986) and (**b**) Fe_{HRT}/Fe_{TOT} ratios (after Ku *et al*. 2008).

Fig. 4. Field photographs of the Gaskiers (**a**–**c**) and Mall Bay Formations (**d**, **e**): (**a**) palaeosols of upper Gaskiers Formation under Drook Formation north of Harbour Main; (**b**) red tillites of middle Gaskiers Formation west of St. Mary; (**c**) scoriaceous volcanic bomb in basal tillite of Gaskiers Formation west of St. Mary; (**d**, **e**) interbedded siltstone and shale with ripple marks in the upper Mall Bay Formation west of St. Mary. Hammer handles in (**c**)–(**e**) are 25 cm long.

Diamictite fabric

Diamictite is massive compared with interbedded shaly and sandy beds within the Gaskiers Formation (Fig. 6a). In thin section diamictite is very poorly sorted (Fig. 7a), with even proportions of sand-, silt- and clay-sized grains. Only 7% by volume is granule or larger grains (Fig. 8d; Table 1) that are matrix supported (Fig. 6c). The archaic term 'boulder clay' is a fair description for this fabric of much of the Gaskiers Formation. The diamictites are generally devoid of bedding (Eyles & Eyles 1989), and show prominent prismatic jointing vertical to basal contacts in some localities (Fig. 6a). In contrast, shaly and silty parts of the formation show clear (Fig. 6b) to fine bedding (Fig. 7c). Large clasts in the diamictite are up to 80 cm long, and include granite, diorite, granophyre, basalt, basaltic scoria, chert, sandstone, siltstone, and shale (Eyles & Eyles 1989). Some clasts in the diamictite are angular, faceted and striated (Brückner & Anderson 1971; Williams & King 1979), but many are rounded (Eyles & Eyles 1989). Sand-size garnet grains in the diamictite are angular and fresh in appearance, and about 9% of them show microscopic chatter-mark gouges (Gravenor 1980).

Also notable are moderately deformed large clasts of soft sediment, such as laminated dolomicrite clasts, up to 2.07 m long and 0.43 m thick, oriented horizontally, vertically, and at various angles in diamictite at Harbour Main (Fig. 6c; Myrow & Kaufman 1999). Even larger clasts in diamictite, tens of metres long, are sediment rafts of gritty sandstone, with overturned folds at their lower margins (Eyles & Eyles 1989).

Table 1. *Petrographic textures (vol%) of palaeosols in the Gaskiers Formation*

Pedotype	Horizon	Sample	Gravel	Sand	Silt	Clay	Soil fabric	Soil texture
Above	Tillite	R3959	6.8	34.4	31.8	27.0	Granular intertextic	Sandy clay loam
Peter	A	R3959	0	27.4	33.6	39.0	Clinobimasepic porphyroskelic	Clay loam
Peter	A	R3960	7.4	21.4	32.0	39.2	Clinobimasepic porphyroskelic	Clay loam
Peter	A	R3961	2.0	26.2	33.4	38.4	Skelmosepic porphyroskelic	Clay loam
Peter	By	R3962	1.2	26.8	39.8	32.2	Skelbimasepic porphyroskelic	Clay loam
Peter	By	R3963	1.2	27.6	38.6	32.6	Skelbimasepic porphyroskelic	Clay loam
Peter	C	R3964	1.6	28.2	38.6	31.6	Skelbimasepic porphyroskelic	Clay loam
Peter	A	R3965	1.0	25.4	33.0	40.6	Skelmosepic porphyroskelic	Clay loam
Peter	A	R3966	1.0	25.6	35.8	37.6	Skelmosepic porphyroskelic	Clay loam
Peter	By	R3967	0.4	30.2	34.2	35.2	Clinobimasepic porphyroskelic	Clay loam
Peter	By	R3968	0.4	28.4	37.6	33.6	Skelmosepic porphyroskelic	Clay loam
Peter	C	R3969	0	29.4	36.0	34.6	Skelmosepic porphyroskelic	Clay loam
Paul	A	R3970	1.4	13.8	40.2	44.6	Skelmosepic porphyroskelic	Silty clay
Paul	A	R3971	0	22.2	38.8	39.0	Skelbimasepic porphyroskelic	Clay loam
Paul	C	R3972	2.0	24.0	36.4	37.6	Skelmosepic porphyroskelic	Clay loam
Paul	C	R3973	0.4	21.4	40.8	37.4	Skelmosepic porphyroskelic	Clay loam
Paul	A	R3974	0.2	23.2	36.4	40.2	Skelbimasepic porphyroskelic	Clay loam
Paul	C	R3975	0.6	27.2	39.4	32.8	Skelmosepic agglomeroplasmic	Clay loam
Paul	C	R3976	0	28.2	38.4	33.4	Skelmosepic agglomeroplasmic	Clay loam
Below	Siltstone	R3977	0	28.8	40.8	30.4	Skelmosepic agglomeroplasmic	Clay loam
Upper	Dolostone	R4058	0	57.6	25.0	17.4	Crystic porphyroskelic	Sandy loam
Lower	Dolostone	R4058	0	54.0	27.2	18.8	Crystic porphyroskelic	Sandy loam
Above	Siltstone	R4060	0	21.2	43.4	35.4	Argillasepic agglomeroplasmic	Clay loam
Above	Siltstone	R4061	0	26.0	34.6	39.4	Insepic agglomeroplasmic	Clay loam
Peter	A	R4062	0	29.6	35.2	35.2	Insepic agglomeroplasmic	Clay loam
Peter	A	R4063	2.8	31.8	34.0	33.4	Insepic agglomeroplasmic	Clay loam
Peter	By	R4064	0	25.8	41.0	33.2	Argillasepic agglomeroplasmic	Clay loam
Peter	By	R4065	0	20.8	43.2	36.0	Argillasepic agglomeroplasmic	Clay loam
Peter	C	R4066	3.4	33.8	33.8	29.0	Isotic intertextic	Clay loam
Above	Sandstone	R4067	2.0	53.0	16.8	28.2	Argillasepic porphyoskelic	Sandy clay loam
Gorman	A	R4068	0	36.8	27.2	36.0	Insepic agglomeroplasmic	Clay loam
Gormanl	C	R4069	0	48.2	26.4	25.4	Argillasepic intertextic	Clay loam
Above	Siltstone	R4070	0	45.0	27.6	27.4	Argillasepic intertextic	Clay loam
Paul	A	R4071	0	32.4	32.8	34.8	Insepic agglomeroplasmic	Clay loam
Paul	A	R4072	0	32.0	37.6	30.4	Insepic agglomeroplasmic	Clay loam
Paul	A	R4073	0	32.6	37.6	29.8	Insepic agglomeroplasmic	Clay loam
Paul	C	R4074	0	7.0	46.0	47.0	Insepic agglomeroplasmic	Silty clay

All samples are shown in Figure 7. Volumes are from counting 500 points in petrographic thin sections perpendicular to bedding using a Swift automated stage and counter. Error is ±2% for common (>10%) components (Murphy 1983).

Shaly and silty beds of the Gaskiers Formation have scattered lonestones up to 11 cm in length (Fig. 8d), which are mostly scoriaceous or massive basalt, like boulders in the diamictite (Fig. 4c). Some oversized clasts deform underlying shaly layers as if they were dropstones (Brückner & Anderson 1971; Williams & King 1979).

Colour and oxidation

The Gaskiers Formation is red in colour (Munsell 10R) and has half or more (molar) of its iron in the oxidized valence state (Fig. 8). Its diamictites generally have an entirely red matrix, contrasting with clasts of black, white, grey and green volcanic, igneous and sedimentary rocks. Siltstones and sandstones are chemically similar, with many igneous rock fragments in which iron is in an unreactive reduced form (Fig. 7a), so that oxidized iron is mostly within the matrix. Supplementary information of Canfield *et al*. (2007) lists pyrite weight per cent in the Gaskiers Formation at Harbour Main averaging 0.01 ± 0.01 wt% (range 0.001–0.06 wt%) and near St. Mary averaging 0.04 ± 0.05 wt% (range 0.001–0.06 wt%), as well as low Fe_{HR}/Fe_{TOT} ratios of 0.31 ± 0.05 (range 0.23–0.43) at Harbour Main and 0.38 ± 0.06 (range 0.23–0.43) at St. Mary (Fig. 2). These results are comparable with molar values reported here (Fig. 8; Table 2), and indicate that oxidation is from matrix hematite or iron hydroxides, but reduced iron is mainly within volcanic rock fragments. Redeposited clasts of red claystone within grey sandstone are evidence that this chemical iron oxidation was during original sedimentation and pre-burial diagenesis (Gravenor 1980), although its degree of redness (Munsell hue) may have been enhanced by burial recrystallization of ferric hydroxides (Retallack 1997). Cambrian (*c*. 525 Ma) prehnite–pumpellyite-facies metamorphism as a result of regional deformation of 6.5 km of overlying shaly rock (Papezik 1974) was not oxidizing, and has reset palaeomagnetic directions of Gaskiers Formation hematite and magnetite (Gravenor *et al*. 1982).

Carbon and sulphur geochemistry

Organic carbon content of the Gaskiers Formation is low (<0.4 wt%), with the exception of one calcareous horizon with

Table 2. *Petrographic composition (vol%) of palaeosols in the Gaskiers Formation*

Pedotype	Formation	Pedotype	Quartz	Feldspar	Clay	Opaque minerals	Mica	Dolomite	Rock fragments	Other
Above	Tillite	R3959	23.6	19.6	27.2	7.4	1.2	3.8	17.0	0.2
Peter	A	R3959	24.2	22.6	41.8	5.6	2.0	0	3.6	0.2
Peter	A	R3960	19.8	21.2	40.2	4.8	2.4	0	11.6	0
Peter	A	R3961	22.6	22.4	38.6	3.4	1.8	0	11.2	0
Peter	By	R3962	25.4	26.8	32.4	2.8	2.0	0.6	9.8	0.2
Peter	By	R3963	22.4	22.6	32.2	5.8	1.0	0	16.0	0
Peter	C	R3964	22.4	24.2	33.2	4.2	1.0	0	15.0	0
Peter	A	R3965	22.8	25.4	39.6	4.0	0.6	0	7.6	0
Peter	A	R3966	22.2	22.8	38.0	4.0	2.4	0	10.6	0
Peter	By	R3967	23.4	26.2	36.2	1.8	3.0	0	9.4	0
Peter	By	R3968	26.6	28.0	33.6	2.4	1.8	0	7.6	0
Peter	C	R3969	25.4	27.0	35.8	2.6	1.4	0	7.8	0
Paul	A	R3970	20.2	25.2	43.0	3.6	1.8	0	6.2	0
Paul	A	R3971	21.2	24.2	37.4	4.8	0.6	0	11.8	0
Paul	C	R3972	20.6	25.8	38.4	2.4	1.4	0	11.4	0
Paul	C	R3973	20.8	24.2	37.8	5.8	1.8	0	9.6	0
Paul	A	R3974	20.8	24.2	41.4	4.4	1.2	0	8.0	0
Paul	C	R3975	25.0	28.0	35.6	2.8	0.4	0	8.2	0
Paul	C	R3976	25.6	28.2	33.4	2.2	0.6	0	10.0	0
Below	Siltstone	R3977	26.2	22.2	31.4	3.4	0.8	0.4	15.6	0
Upper	Dolostone	R4058	2.6	2.2	2.6	8.6	0	55.2	12.2	16.6
Lower	Dolostone	R4058	3.6	1.8	1.6	7.4	0	51.8	15.6	18.2
Above	Siltstone	R4060	16.4	15.0	35.0	7.0	0.8	0	25.8	0
Above	Siltstone	R4061	23.0	21.0	39.4	4.8	0.4	3.6	7.8	0
Peter	A	R4062	22.0	24.8	35.6	5.2	3.2	0.4	8.8	0
Peter	A	R4063	18.4	21.8	34.4	7.0	1.2	1.6	15.6	0
Peter	By	R4064	23.8	27.0	33.2	3.2	3.6	0	9.2	0
Peter	By	R4065	24.0	25.0	34.6	3.8	1.8	0.8	10.0	0
Peter	C	R4066	25.0	25.2	31.6	6.0	1.4	1.0	9.8	0
Above	Sandstone	R4067	23.2	25.2	30.0	6.4	5.2	0	10.0	0
Gorman	A	R4068	25.6	22.6	35.2	6.0	3.8	0	6.8	0
Gormanl	C	R4069	29.2	29.8	23.6	3.2	4.4	0	9.8	0
Above	Siltstone	R4070	22.4	24.6	28.8	6.4	2.6	0	14.4	0
Paul	A	R4071	26.0	21.0	35.0	4.0	3.6	0	10.4	0
Paul	A	R4072	21.4	15.2	33.6	5.6	4.2	0	19.8	0
Paul	A	R4073	23.2	23.8	29.6	4.2	2.8	0	16.4	0
Paul	C	R4074	17.0	25.8	27.4	3.0	0.8	0	3.6	22.4

All samples are shown in Figure 7. Volumes are from counting 500 points in petrographic thin sections cut perpendicular to bedding using a Swift automated stage and counter. Error is ±2% for common (>10%) components (Murphy 1983). Other in most cases is mafic minerals, but for R4058 it is dolomicrite.

3.12 wt% organic carbon (Fig. 8b; Table 2). Supplementary data of Canfield *et al*. (2007) support this observation: carbon weight per cent in the Gaskiers Formation at Harbour Main averages 0.024 ± 0.037 wt% (range 0.001–0.06 wt%) and near St. Mary averages 0.034 ± 0.033 wt% (range 0.001–0.06 wt%). Nevertheless, there is more carbon than pyrite sulphur, and corresponding C/S ratios average 4.84 ± 8.63 (range 0.001–30.0) for Harbour Main and 4.62 ± 8.17 (range 0.008–25.0) for St. Mary (Fig. 2). Sulphur isotopic compositions in pyrite of the Gaskiers Formation are generally positive: only six out of 23 analyses are negative, and $\delta^{34}S_{CDT}$ values average +2.27 ± 10.00‰ (range –12.31 to +18.08‰) for Harbour Main and +7.49 ± 12.07‰ (range –12.26 to +26.35‰) for St. Mary (Canfield *et al*. 2007). Carbon and oxygen isotopic values from large dolomicrite clasts in the upper Gaskiers Formation near Harbour Main are both unusually depleted (Myrow & Kaufman 1999): $\delta^{13}C_{PDB}$ values average –5.04 ± 1.78‰ (range –1.7 to –7.8‰) and $\delta^{18}O_{PDB}$ values average –18.07 ± 0.29‰ (range –17.2 to –18.5‰).

Bedding and ripple marks

Few sedimentary structures are present within thick diamictite beds and silty interbeds (Fig. 6a) of the Gaskiers Formation (Williams & King 1979), but there is a variety of graded beds, asymmetric ripples, lenticular beds (sandy ripple trains in clayey matrix), flaser beds (clay-filled inter-ripple depressions) and wavy beds (closely alternating shale and silty ripples with local truncations) in the underlying Mall Bay and overlying Drook formations (Fig. 4d and e; Gardiner & Hiscott 1988). Some of the massive appearance of siltstones of the Gaskiers Formation is misleading, because thin sections reveal finely laminated varve-like beds with minor vertical disruption (Fig. 7c) and layering deformed by growth of sand crystals (Fig. 7d and e).

Volcanic features

Radiometric dating of the Harbour Main Volcanics to the east and north (O'Brien *et al*. 2001) and Marystown Volcanics to the west

Table 3. *Chemical analyses (wt%) and bulk density (g cm^{-3}) of beds (Mall Bay Formation) and palaeosols (Gaskiers Formation)*

Pedo-type	Sample	SiO_2	Al_2O_3	Fe_2O_3	FeO	CaO	MgO	Na_2O	K_2O	Cr_2O_3	TiO_2	MnO	P_2O_5	SrO	BaO	LOI	C	Total	Density (g cm^{-3})
Bed	R3956	74.12	11.83	3.09	2.14	0.70	1.36	1.57	4.29	0.03	0.45	0.08	0.208	0.01	0.14	2.03	0.02	99.91	2.65
Bed	R3957	73.25	11.65	2.96	1.92	0.65	1.42	1.91	3.78	0.03	0.44	0.07	0.157	0.01	0.09	2.18	0.04	98.61	2.64
Bed	R3958	73.53	12.52	3.45	2.38	0.72	1.13	3.35	2.81	<0.01	0.46	0.09	0.12	0.02	0.05	1.78	0.02	99.98	2.60
Bed	R3965	65.46	15.56	3.86	1.95	0.79	1.88	2.29	4.89	0.02	0.67	0.06	0.146	0.01	0.08	3.40	0.43	99.11	2.66
Peter	R3966	64.41	15.74	4.36	2.28	0.69	2.01	2.11	5.02	0.01	0.66	0.07	0.143	0.01	0.10	3.55	0.03	98.88	2.67
Peter	R3967	64.39	15.82	4.30	2.34	0.74	2.06	2.12	5.08	<0.01	0.70	0.08	0.15	0.01	0.09	3.59	0.03	99.14	2.65
Peter	R3968	63.18	16.1	5.48	2.61	0.65	2.37	2.13	5.09	0.01	0.72	0.09	0.149	0.01	0.08	3.94	0.03	100.0	2.68
Peter	R3969	63.25	15.81	5.32	2.59	0.65	2.27	2.06	5.08	<0.01	0.71	0.08	0.15	0.01	0.08	3.89	0.02	99.36	2.64
Peter	R3970	64.56	15.52	4.56	2.08	0.64	2.04	1.83	5.32	0.02	0.67	0.08	0.136	0.01	0.13	3.63	0.03	99.14	2.65
Paul	R3971	65.66	15.44	4.50	2.14	0.62	2.06	2.13	4.93	<0.01	0.68	0.08	0.144	0.01	0.09	3.61	0.03	99.96	2.66
Paul	R3972	65.83	15.15	4.65	2.07	0.57	1.97	1.67	5.2	<0.01	0.66	0.07	0.132	0.01	0.11	3.66	0.02	99.68	2.65
Paul	R3973	65.04	15.49	5.04	2.48	0.78	2.13	2.26	4.69	0.01	0.77	0.08	0.153	0.01	0.07	3.46	0.03	99.99	2.65
Paul	R3974	64.36	15.72	4.60	2.21	0.76	2.03	2.37	4.84	<0.01	0.67	0.08	0.158	0.01	0.11	3.48	0.04	99.23	2.65
Bed	R4061	66.07	15.38	4.31	1.17	1.46	1.74	2.69	4.52	0.01	0.57	0.07	0.117	0.02	0.21	2.87	0.14	100.05	2.69
Peter	R4062	64.28	16.15	4.76	1.04	0.86	1.76	2.48	5.04	0.01	0.63	0.06	0.116	0.02	0.15	2.63	0.03	98.95	2.72
Peter	R4063	62.90	16.71	4.82	0.78	0.88	1.68	2.57	5.28	<0.01	0.66	0.06	0.116	0.02	0.19	2.82	0.05	98.70	2.72
Peter	R4064	67.09	15.03	4.54	0.91	0.77	1.63	2.61	4.43	<0.01	0.58	0.08	0.113	0.01	0.13	2.34	0.02	99.36	2.66
Peter	R4065	64.06	16.31	4.69	0.84	0.86	1.71	2.38	5.04	<0.01	0.65	0.05	0.118	0.01	0.14	2.77	0.02	98.80	2.67
Peter	R4066	61.20	16.48	5.66	0.91	1.56	1.65	2.49	5.15	0.01	0.76	0.06	0.162	0.02	0.26	3.23	0.16	98.69	2.74
Peter	R4068	66.09	13.95	5.30	3.00	0.77	2.84	2.39	2.93	0.02	0.70	0.12	0.072	0.02	0.06	3.02	0.01	98.27	2.70
Peter	R4069	67.52	14.07	4.91	2.53	0.81	2.63	2.69	2.81	0.01	0.75	0.11	0.088	0.02	0.08	2.85	0.01	99.35	2.68
Paul	R4071	66.83	14.86	4.90	2.09	0.55	1.93	3.65	2.71	0.01	0.53	0.10	0.053	0.02	0.08	2.49	0.01	98.71	2.70
Paul	R4072	68.99	13.62	4.67	2.33	0.54	2.09	3.51	2.16	<0.01	0.49	0.11	0.062	0.02	0.08	2.37	0.01	98.72	2.70
Paul	R4073	70.81	13.63	4.31	1.95	0.58	1.83	3.73	2.13	0.01	0.48	0.09	0.052	0.02	0.10	2.15	0.02	99.97	2.68
Paul	R4074	48.89	10.75	3.40	1.82	14.54	1.74	3.81	0.99	<0.01	0.48	0.38	0.168	0.01	0.04	13.4	3.12	98.60	2.68
Error	All	0.1	0.0.08	0.0.03	0.09	0.04	0.54	0.05	0.02		0.003	0.001	0.004	.0012	.0005				0.04

Specimen locations are shown in Figure 7. Analyses are by XRF, with FeO by Pratt titration and C by Walkley–Black tritration from ALS Chemex of Vancouver, BC, Canada, using Canadian Certified Reference Materials Project standard SY-4. Errors (2σ) are from 89 replicate analyses. LOI, loss on **ignition.

Table 4. *Pedotypes of the Gaskiers Formation*

Pedotype	Diagnosis	Soil Survey Staff (2010)	Food & Agriculture Organization (1974)	Australian (Isbell 1996)
Gorman	Green–red mottled sandstone with relict bedding	Psamment	Fluvisol	Stratic Rudosol
Paul	Red–green mottled surface (A) horizon over bedded clayey subsurface (Bw) horizon	Eutrudept	Eutric Cambisol	Lutic Rudosol
Peter	Red–green mottled surface (A) over subsurface horizon (By) with gypsum sand crystal casts	Haplogypsid	Gypsic Xerosol	Hypersalic Rudosol

Table 5. *Pedotype interpretation of the Gaskiers Formation*

Pedotype	Climate	Organisms	Topographic setting	Parent material	Time for formation (years)
Gorman	Not diagnostic of climate	Microbial soil crust	Near-stream sand bar	Quartzo-feldspathic sand	5–100
Paul	Humid temperate (6.9 ± 4.4 °C MAT and 1069 ± 182 mm MAP at St. Mary, and 6.3 ± 4.4 °C MAT and 825 ± 182 mm MAP at Harbour Main)	Microbial soil crust	Well-drained alluvial terrace	Quartzo-feldspathic sand	1000–6000
Peter	Humid temperate (6.9 ± 4.4 °C MAT and 1016 ± 182 mm MAP at St. Mary, and 6.1 ± 4.4 °C MAT and 922 ± 182 mm MAP at Harbour Main)	Microbial soil crust	Well-drained alluvial terrace	Quartzo-feldspathic sand	10000–12000

Interpretations are discussed in text. MAT, mean annual temperature; MAP, mean annual precipitation.

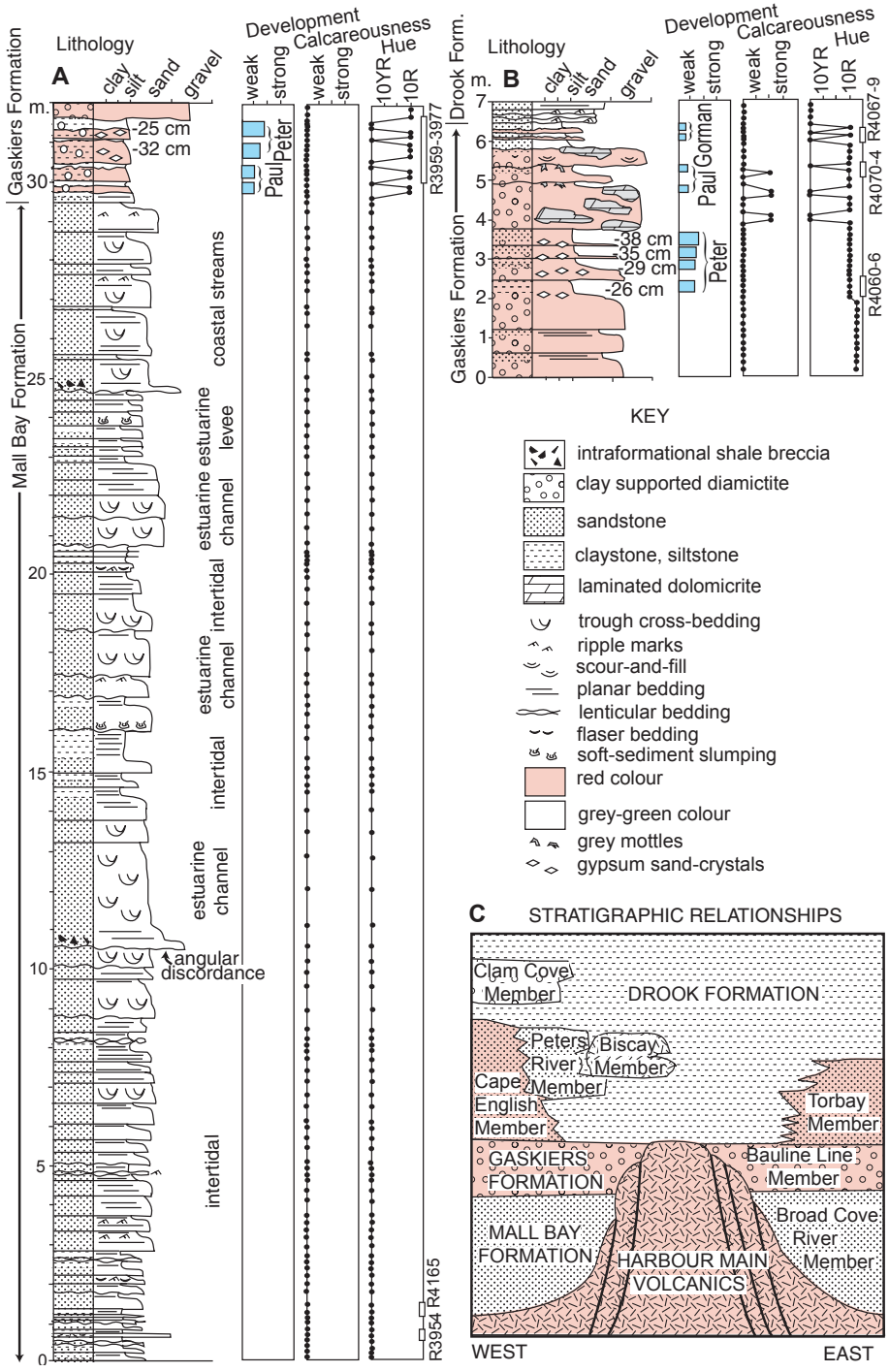

Fig. 5. Measured sections with palaeosols in the Gaskiers Formation at St. Marys (**a**) and Harbour Main (**b**), with stratigraphic relationships of the Gaskiers Formation (**c**; after King 1988). Palaeosol thickness is shown by boxes whose width corresponds to degree of development. Scales of development and calcareousness from field application of dilute acid follow Retallack (1997), and colours are from a Munsell chart (online version).

(Rabu *et al*. 1993) provides evidence of active volcanism during the 580–581 Ma time span of zircon in volcanic ash of the Gaskiers Formation (Bowring *et al*. 2003). Coeval volcanic activity is also indicated by volcanic bombs and lapilli in the Gaskiers Formation (Gravenor 1980). In thin section some quartz grains have the characteristic bipyramidal form and embayments of volcanic quartz (Fig. 9f).

Palaeopedological observations

The following observations of soil-like features in the Gaskiers Formation are offered without interpretation beyond whether they were originally soils, as opposed to sedimentary, metamorphic, hydrothermal, or tectonic features. These features confirm and amplify the array of features useful for identifying palaeosols in sedimentary sequences geologically older than the evolution of plant roots (Retallack 2011*a*, *b*, 2012*a*, *b*).

Soil horizons

Silty and shaly intervals within the Gaskiers Formation show alternating horizons of grey and red colour, with the central part of erosionally bounded beds red, but tops or bottoms grey (Figs 6a and 8d). In addition to drab-coloured clasts, there are also mottles of grey–green siltstone and claystone in matrix of the same grain size,

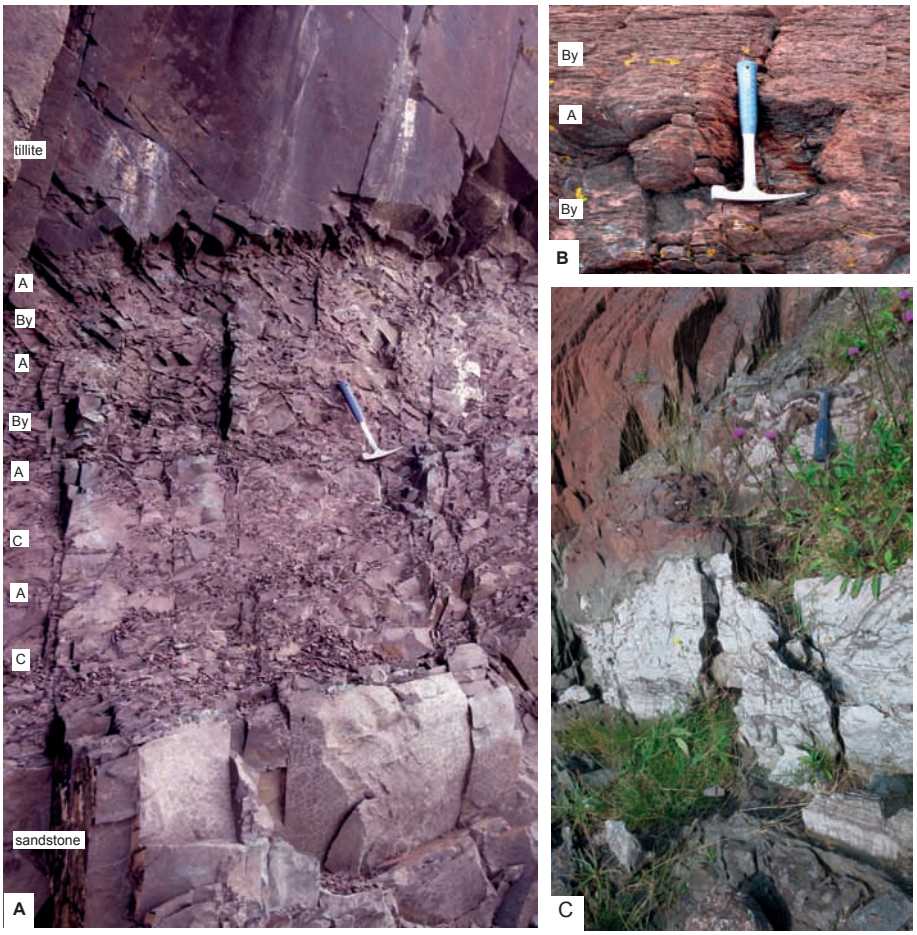

Fig. 6. Palaeosols of the Gaskiers Formation: (**a**) sequence of palaeosols in basal Gaskiers Formation west of St. Mary; (**b**) Peter pedotype in upper Gaskiers Formation north of Harbour Main; (**c**) weathered blocks of micritic dolomite in upper Gaskiers Formation north of Harbour Main. Hammer handles are 25 cm long.

and dispersed layers of light-coloured sand crystals (Fig. 6b). These gradational and diffuse contacts are different from graded beds examined in the Mall Bay Formation, with their pervasive lamination and ripple marks (Fig. 4d and e; Gardiner & Hiscott 1988). The grey graded beds of the Mall Bay Formation have thick very clayey upper parts, and very sandy lower parts, whereas red siltstone sequences have a more even mix of sand, silt and clay throughout the profile (Fig. 8). Mall Bay Formation graded beds have concave grain-size profiles like those of turbidites of the Ediacaran Poudinge de Granville, France (Eyles 1990), whereas beds identified here as palaeosols in the Gaskiers Formation have convex grain-size profiles, like palaeosols of the Ediacara Member of the Rawnsley Quartzite of South Australia (Retallack 2012*a*). Mechanistic explanations for these distinct grain-size profiles are (1) clay settling from suspension in a turbidite or graded bed, but (2) clay formed by chemical weathering in a palaeosol. Such a model of progressive soil formation also explains why palaeosols in the Gaskiers Formation that are more clayey toward the surface also show greater destruction of primary bedding (Fig. 8) and geochemical differentiation (Fig. 10).

These surface horizons slightly more clayey and carbonaceous than subsurface surface horizons are A horizons in soil science terminology (Soil Survey Staff 2010). These are all simple profiles with no discernible subsurface accumulation of clay (Fig. 8). Nevertheless, subsurface horizons are oxidized and also chemically weathered and qualify as Bw horizons. Other profiles have subsurface accumulations of sand crystals after salts (Figs 6b and 7d, e), and so are By horizons of Soil Survey Staff (2010).

Soil structures

Sequences identified in the field as palaeosols in the Gaskiers Formation have bedding disrupted by a distinctive system of hackly joints (Fig. 6a and b), like soil clods (peds) and their irregular bounding planes of alteration (cutans) diagnostic of soils (Retallack 1997). In thin section, these natural aggregates of matrix (blocky peds) are divided by an irregular network of illuviated and oxidized clay (sesquiargillans; Fig. 7b); in other words, the soil dilated and cracked allowing oxidation and clay films to coat the soil clods. This process is physically impossible in permanently waterlogged soils, lakes or the sea bed (Buurman *et al*. 1998). Nothing like this was seen in graded beds of the Mall Bay Formation (Fig. 4d and e), where primary sedimentary structures of tempestites, tidalites, and turbidites are well preserved (Fig. 4d and e).

Sand crystals are also diagnostic soil structures of desert soils, and grow in optical continuity around existing framework grains (Dan *et al*. 1973; Dan & Yaalon 1982; Lebron *et al*. 2009). In contrast, evaporitic sedimentary sulphates have clean crystals without inclusions, displacing sedimentary matrix or forming thick evaporite beds (Ziegenbalg *et al*. 2010). Sand crystals of the Gaskiers Formation do not retain any evaporite mineral, like pseudomorphous sand crystals in other Ediacaran palaeosols (Retallack 2012*a*, *b*). Furthermore, the original minerals of sand crystals in the Gaskiers Formation are uncertain because the crystals were degraded by partial dissolution and successive fill of the mineral cavity (Fig. 7d and e), as is best known from halite hopper casts (Brooks 1955). Halite, barite and gypsum are well-known

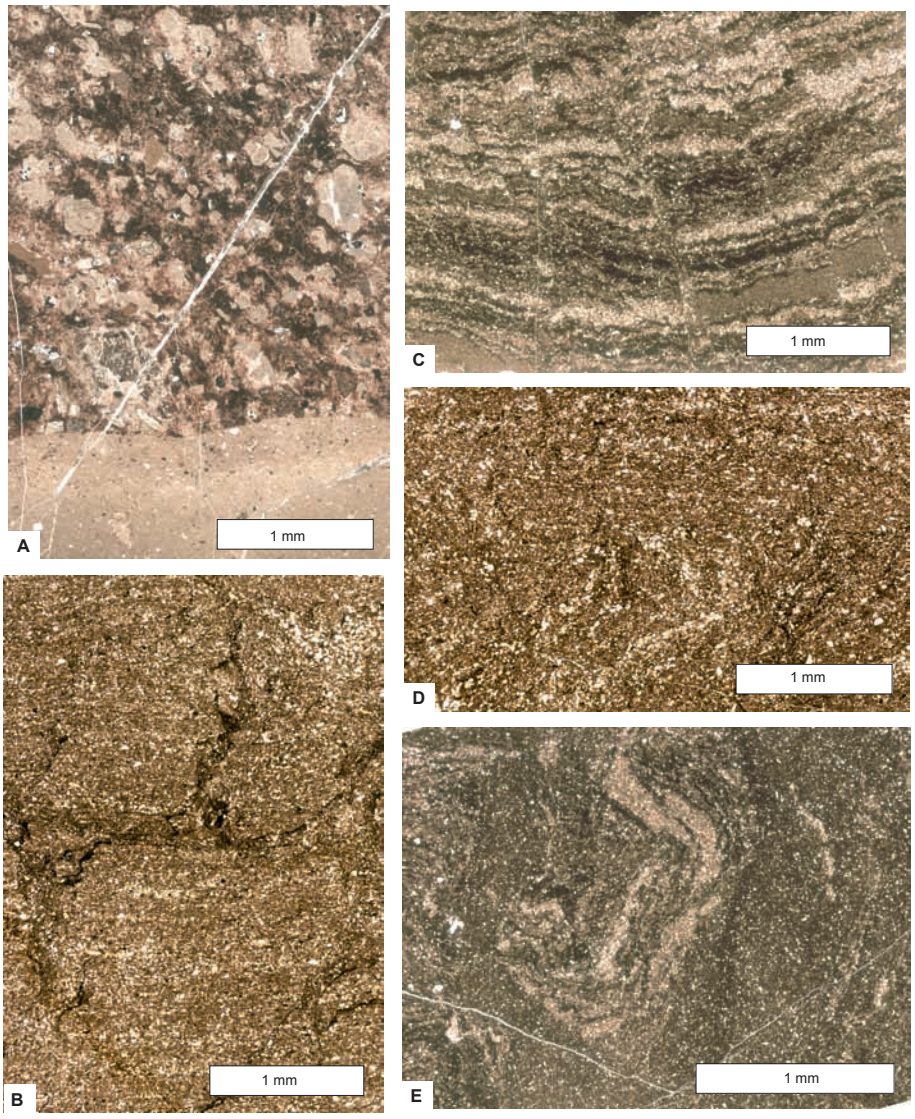

Fig. 7. Petrographic thin sections of palaeosols of the Gaskiers Formation of Newfoundland west of St. Mary (**a**) and north of Harbour Main (**b**–**e**): (**a**) tillite overlying A horizon of Peter pedotype west of St. Mary; (**b**) clay skins defining fine blocky peds in Bw horizon Paul pedotype; (**c**) crenulated lamination in A horizon of Peter pedotype; (**d**) disrupted bedding in A horizon of Paul pedotype; (**e**) gypsum sand crystal in By horizon of Peter pedotype. All images are from a slide scanner from slides cut vertical to bedding and oriented with upper side to top. Sample numbers in Museum of Natural and Cultural History of the University of Oregon are R3960 (**a**), R4072 (**b**), R4061 (**c**), R4071 (**d**), R4064 (**e**).

pedogenic salts (Retallack & Huang 2010). The radiating form of some Gaskiers Formation sand crystals could be remnants of corroded gypsum (Fig. 7d and e).

Microscopic soil structures are also revealed in thin section, particularly the partial dissolution of feldspar grains (Fig. 9d) and rock fragments (Fig. 9e), owing to chemical weathering. Also notable is the appearance of fine-grained portions of soil matrix when viewed under crossed Nicols, showing patches and sheets of highly oriented (high-birefringence) clays among regions of poorly oriented clays (Fig. 9d–f; Table 1). The technical term for this is sepic plasmic fabric, which is thought to form by highly deviatoric local stresses in a regime of overall volume change unique to soils (Brewer 1976).

Chemical weathering

The master equation for weathering in soils is hydrolysis: the incongruent dissolution of feldspar and other weatherable minerals by carbonic acid to form clay and release nutrient cations (Ca^{2+}, Mg^{2+}, Na^{+}, K^{+}). Hydrolytic alteration is revealed by increased clay detected by point counting and molar ratios of alumina/bases determined by chemical analysis towards the tops of profiles and in profiles with less distinct bedding compared with thin-bedded profiles (Fig. 8). Groundwater or hydrothermal water cannot produce such cationic depletion unless it has a comparable source of acid, such as volcanic exhalation of CO_2 (Little & Lee 2006) or oxidation of abundant pyrite (Nordstrom 2003). Volcano-hydrothermal veining is unknown (Williams & King 1979; Eyles & Eyles 1989), and pyrite is very rare in the Gaskiers Formation (Canfield *et al*. 2007).

Chemical index of alteration (CIA) calculated for sedimentary rocks demonstrates a general level of basinal hydrolysis useful for distinguishing glacial (CIA <55) from non-glacial (CIA >70) conditions (Passchier & Krissek 2008). The upper Mall Bay Formation tidalite had CIA 57.4 ± 1.3 (three analyses), whereas the Gaskiers red beds of St. Marys had CIA 60.7 ± 2.6 (10 analyses) and upper Gaskiers red beds of Harbour Main had CIA 59.3 ± 1.7 (11 analyses; all errors 1SD). These are marginally glacial to cold-temperate CIA values, comparable with those calculated for the non-glacial Mesoproterozoic middle Appekunny, Snowslip and McNamara Formations of Montana (Gonzàlez-Àlvarez & Kerrich 2012), terrestrial Cryogenian (Marinoan) glacial deposits of the Ayn Formation of Oman (Rieu *et al*. 2007), and the Ediacaran Boston Bay Group of Massachusetts (Passchier & Erukanure 2010). A variety of complications for interpretation of CIA have been outlined by Bahlburg & Dobrzinksi (2011) and Gonzàlez-Àlvarez & Kerrich

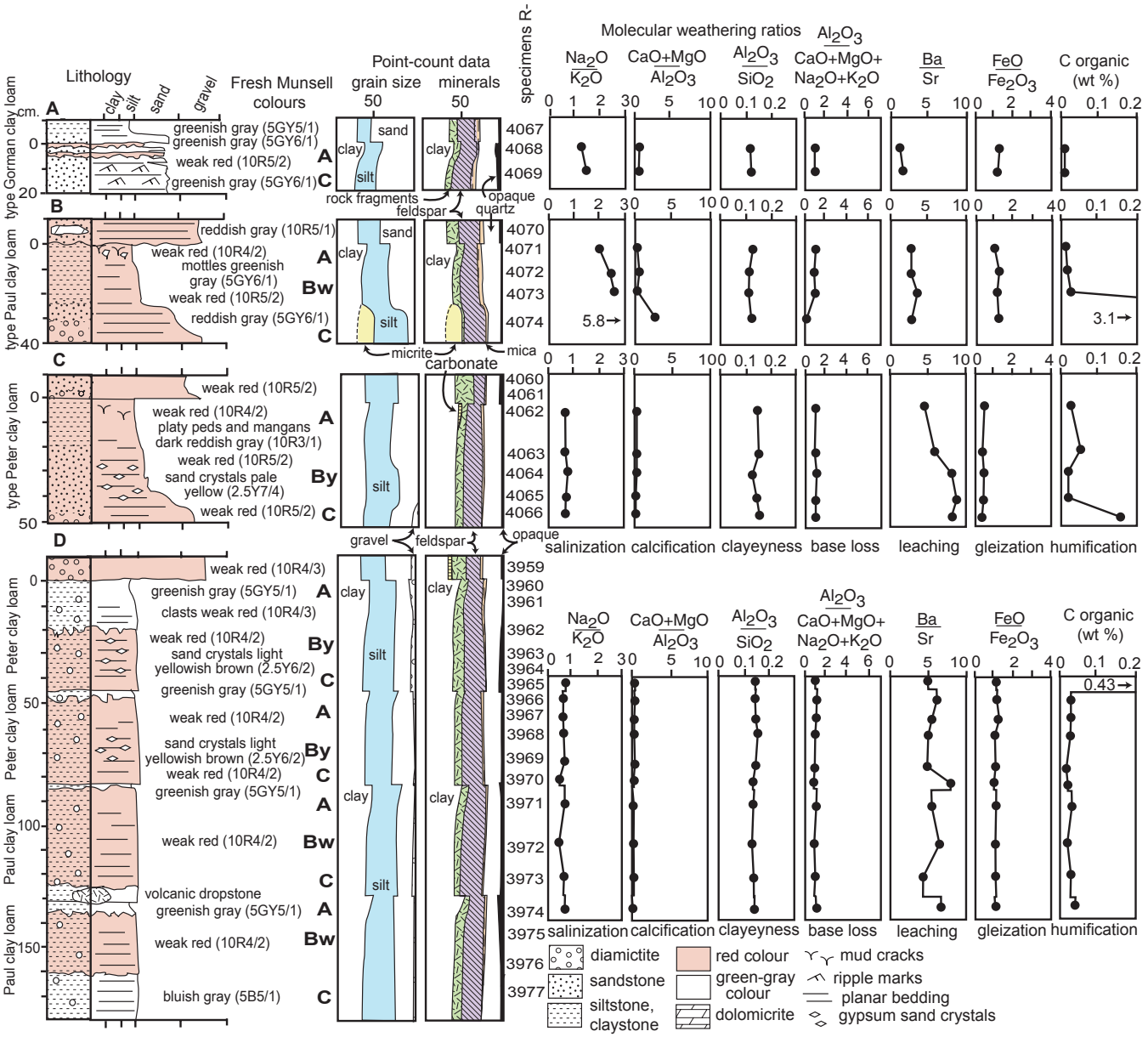

Fig. 8. Grain size and mineral (from point-counting) and chemical composition (from XRF) of palaeosols in the Gaskiers Formation of Newfoundland. Molar weathering ratios are designed to reveal degree of common soil-forming reactions, such as base loss (Retallack 1997).

(2012), especially source region reworking and climatic seasonality. Varve-like sediments (Fig. 7c) may indicate snowy winters (Retallack & Jahren 2008), but that is a minor effect compared with tropical monsoons (Gonzàlez-Àlvarez & Kerrich 2012), which are unlikely for the palaeolatitude (34° ± 8°S) of the Gaskiers Formation (Evans & Raub 2011; Pisarevsky *et al*. 2012; Thompson *et al*. 2012). Redeposition of deeply weathered soils by large rivers of cratons is also unlikely in the active volcanic source terrane, with short streams and cool-temperate lowland palaeoclimate envisaged for the Gaskiers Formation (Rabu *et al*. 1993; Landing 1996; McNamara *et al*. 2001; O'Brien *et al*. 2001; Ichaso *et al*. 2007).

The progress of hydrolysis is revealed more precisely by calculating chemical losses and gains, as well as volume loss and gain to a stable constituent (equations (1) and (2) above, after Brimhall *et al*. 1992). There are four distinct fields of chemical processes revealed by such analysis (Fig. 10), and the field of collapse of volume and loss of cations characteristic of soils is demonstrated by chemical analyses of palaeosols in the Gaskiers Formation. Also plotted in Figure 10 is comparable analysis of a Mall Bay Formation graded bed (tidalite), which falls into the dilation of volume and gain of cations characteristic of sediments. Titanium is mainly within heavy minerals resistant to weathering such as ilmenite, and so is concentrated near the tops of soils as other elements are weathered away. In contrast, heavy minerals settle to the bottom of graded sedimentary beds. Hydrolysis of soils depletes major nutrient cations, as well as silica and alumina, but in marine and aquatic settings these elements are stable or enriched. The behaviour of iron is regulated by redox conditions: enriched in red oxidizing soils like palaeosols of the Gaskiers Formation, but depleted in waterlogged stagnant soils like those of coal measures (Retallack 1997). Geochemical strain and mass balance of single beds thus provides a clear distinction between palaeosols and sediments in the Gaskiers and Mall Bay Formations.

Stable isotope geochemistry

The isotopic composition of soil carbonate and weathered marine limestones is strongly isotopically depleted (negative $\delta^{13}C_{PDB}$ and $\delta^{18}O_{PDB}$), whereas marine limestone is near zero by definition of the analytical standard (PDB, a marine belemnite, or standard mean ocean water, SMOW; Knauth *et al*. 2003; Knauth & Kennedy 2009). Furthermore, oxygen and carbon isotopic compositions of pedogenic carbonate covary strongly in soils because of evaporative effects and enzymatic fractionation during photosynthesis (Ufnar *et al*. 2008). Carbonate clasts in the upper Gaskiers Formation at Harbour Main show strongly depleted values of carbon and oxygen, but little variation in oxygen values compared with carbon values (Myrow & Kaufman 1999). These carbonate clasts are also finely banded unlike pedogenic carbonate. Nevertheless, these marine or aquatic dolomicrites show isotopic compositions compatible with alteration by weathering (Knauth & Kennedy 2009). Their narrow range of oxygen isotopic compositions and prominent recystallization (Fig. 9) may also reflect later prehnite–pumpellyite metamorphic alteration (Papezik 1974; Myrow & Kaufman 1999).

Pyrite is rare in the Gaskiers Formation, and pyrite sulphur isotopic values ($\delta^{34}S_{CDT}$) by Canfield *et al*. (2007) are largely positive, as is usual for igneous and metamorphic pyrite. Only rare small grains of cubic pyrite were seen in thin sections of the palaeosols, and no framboids like those produced by bacteria (Altschuler *et al*. 1983). Very few pyrites in the Gaskiers Formation had the negative sulphur isotopic values created by sulphate-reducing bacteria in salt marsh soils (Altschuler *et al*. 1983) or euxinic ocean basins (Canfield & Farquhar 2009).

Pedotypes

Three distinct kinds of palaeosols found in the Gaskiers Formation are named as pedotypes and based on profiles near Harbour Main (Fig. 8; Table 3). The pedotypes reflect different degrees of destruction of primary bedding features by soil formation: from minimal disruption of bedding in Gorman pedotype, to moderate and shallow disruption of bedding in the Paul pedotype, to more extensive disruption of bedding by small sand crystals in the Peter pedotype. Pedotypes are named as a basis for interpretation (Table 4), but the observation of differing degrees of destruction of sedimentary features on which they are based is in itself an indication that they were created by early diagenetic processes such as soil formation.

Gaskiers glaciation reconsidered

Sedimentological and palaeopedological observations listed above are combined in the following paragraphs to offer a new palaeoenvironmental interpretation of the Gaskiers Formation under the familiar five-factor headings of palaeopedology (Retallack 1997).

Duration of soil formation

Palaeosols of the Gaskiers Formation are weakly to very weakly developed in the development scheme of Retallack (1997), because original bedding is not thoroughly disrupted (Fig. 7b and c), and even sand crystals are small and sparse (Fig. 7d and e). In modern soils formed under vascular land plants these degrees of bedding destruction would represent no more than years or decades of plant growth (Gile *et al*. 1981; Harden 1982), but this gives only lower bounds considering the lack of aggressively rooting plants during the Ediacaran. Sand crystal size and abundance is a better guide to duration of Ediacaran soil formation. In the Arena Valley, Antarctica, salt stage III of gypsum sand-nodules larger than 2 mm over less than 20% surface area (more than Peter pedotype) takes 18–90 ka and a weakly cemented pan takes more than 250 ka (Bockheim 1990; Retallack *et al*. 2001). In the Negev and Atacama deserts also, gypsum hardpans are found in soils millions of years old (Dan & Yaalon 1982; Ewing *et al*. 2006). The relationship between gypsum abundance (*G* in area %) and geological age (*A* in ka) in the Sinai and Negev deserts of Israel (Dan *et al*. 1973; Yaalon *et al*. 1982) is given by the following equation:

$$A = 3.987G + 5.774. \quad (6)$$

This relationship is highly correlated ($R^2 = 0.95$) but has broad standard error of ±15 ka. For the Peter palaeosol at Harbour Main this equation gives 12 ± 15 ka and for Peter palaeosols at St. Mary it yields 11 ± 15 ka and 10 ± 15 ka. These are time frames in which moderately developed soils and ecosystems form today in benign (non-gypsic) environments (Retallack 1997), so that Ediacaran rates of soil development were much slower than modern rates (Table 3). Gypsum accumulation today is limited by cold or lack of water, which excludes most plants in modern environments, so that gypsum accumulates at much slower rates than carbonate in soils (Retallack 2005).

Parent material

Palaeosols of the Gaskiers Formation formed on quartzo-feldspathic till and loess, and in one case (type Paul clay loam) on laminated dolomicrites (Fig. 8). Within the tectonopetrographic scheme of Dickinson & Suczek (1979), the point-counted quartz–feldspar–lithic ratios of Gaskiers Formation palaeosols plot in the area between magmatic arcs and recycled orogens (Fig. 11a). Within the volcanic geochemical scheme of Le Bas *et al*. (1986) Gaskiers palaeosols are rhyolitic, dacitic, trachydacitic, and trachyandesitic (Fig. 11b). Within the granitic geochemical scheme of Middlemost (1994), Gaskiers palaeosols are granitic, granodioritic, quartz monzonitic, and monzonitic (Fig. 11c). These data are compatible with the mix of clasts, including rhyolite, granite, and basalt, found in the tillite (also plotted in Fig. 11a). Soil formation within palaeosols away from these parent materials was toward the quartz–lithic and siliceous compositions of recycled orogens. The source terrain of the Gaskiers Formation was not a small mid-oceanic volcanic arc like the modern Marianas or Antilles (as reconstructed by Ichaso *et al*. 2007, fig. 9), but a complex arc like modern Japan (Fig. 12), including substantial amounts of continental crust (Landing 1996).

Palaeotopography

Palaeosols in the Gaskiers Formation are evidence for a radical revision of its palaeogeography, which has been interpreted as deep marine turbidites (Mall Bay Formation) overlain by deep marine tillites (Gaskiers Formation) by Eyles & Eyles (1989). Abyssal plain and distal submarine fan palaeoenvironments (Ichaso *et al*. 2007) are ruled out by the high rates of sediment accumulation calculated above (0.57 ± 0.49 mm a^{-1} for Gaskiers Formation and 0.16 ± 0.01 mm a^{-1} for Gaskiers–Mistaken Point Formations). Pelagic sediments of the eastern equatorial Pacific Ocean accumulate at rates of 0.002–0.009 mm a^{-1} (Tominaga *et al*. 2011). The Atlantic abyssal plain has similarly low rates of sediment accumulation (0.005 mm a^{-1}), and nearby distal turbidite fans accumulate at rates of only 0.012–0.026 mm a^{-1} (Alibés *et al*. 1999). A North American Cordilleran model of the Conception Group is more appropriate for the high sedimentation rates of the Gaskiers Formation (Nance *et al*. 2002), particularly the Ridge Basin of southern California, which accumulated at an astounding rate of 2.3 mm a^{-1} (Crowell 2003).

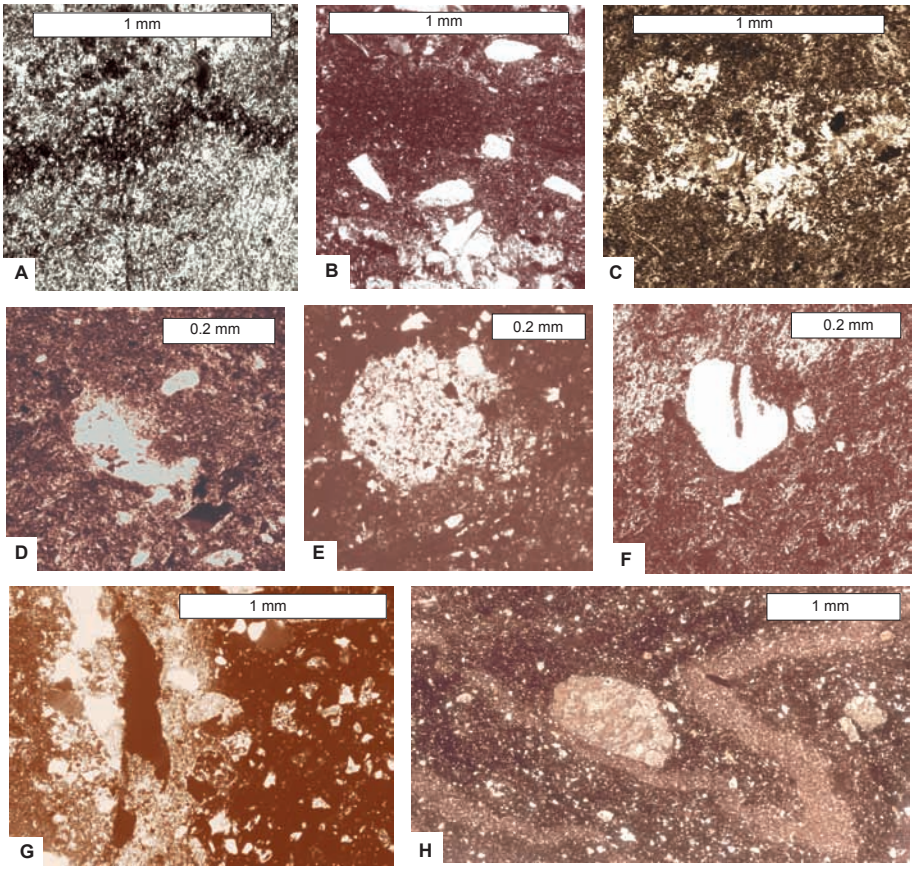

Fig. 9. Petrographic thin sections of palaeosols of the Gaskiers Formation at Harbour Main (**a**, **b**, **d**, **f**, **g**) and St. Mary (**c**, **e**): (**a**) crenulated organic seam in laminated carbonate clast; (**b**) laminated organic matter in A horizon of Gorman pedotype; (**c**) tubular feature comparable with *Prasinema nodosum* Retallack 2011*b*; (**d**) partly dissolved feldspar and insepic plasmic fabric in A horizon Peter pedotype; (**e**) partly dissolved rock fragment and insepic plasmic fabric in By horizon Peter pedotype; (**f**) volcanic quartz and bimasepic plasmic fabric in A horizon Paul pedotype; (**g**) pedotubule with carbonate sheath in C horizon Peter pedotype; (**h**) soft sediment deformation in By horizon Peter pedotype. Sample numbers in Museum of Natural and Cultural History of the University of Oregon are R4058 (**a**), R4068 (**b**), R3961 (**c**), R4063 (**d**), R3971 (**e**), R4066 (**f**), R4063 (**g**). All thin sections cut perpendicular to bedding and oriented with upper surface to top.

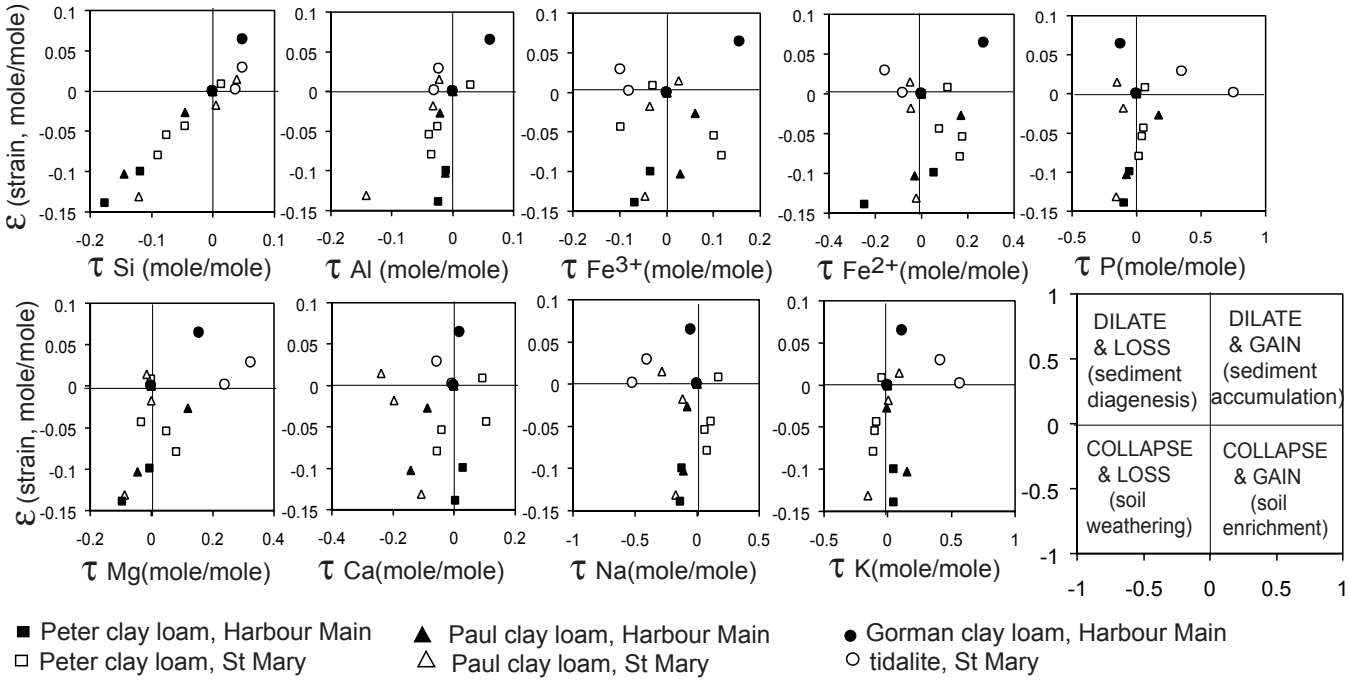

Fig. 10. Mass-balance geochemistry of palaeosols in the Gaskiers Formation of Newfoundland, including estimates of strain from changes in an element assumed stable (Ti) and elemental mass transfer with respect to an element assumed stable (Ti, following Brimhall *et al*. 1992). Zero strain and mass transfer is the parent material lower in the profile; higher horizons deviate from that point owing to soil formation or sedimentation as indicated in key to lower right.

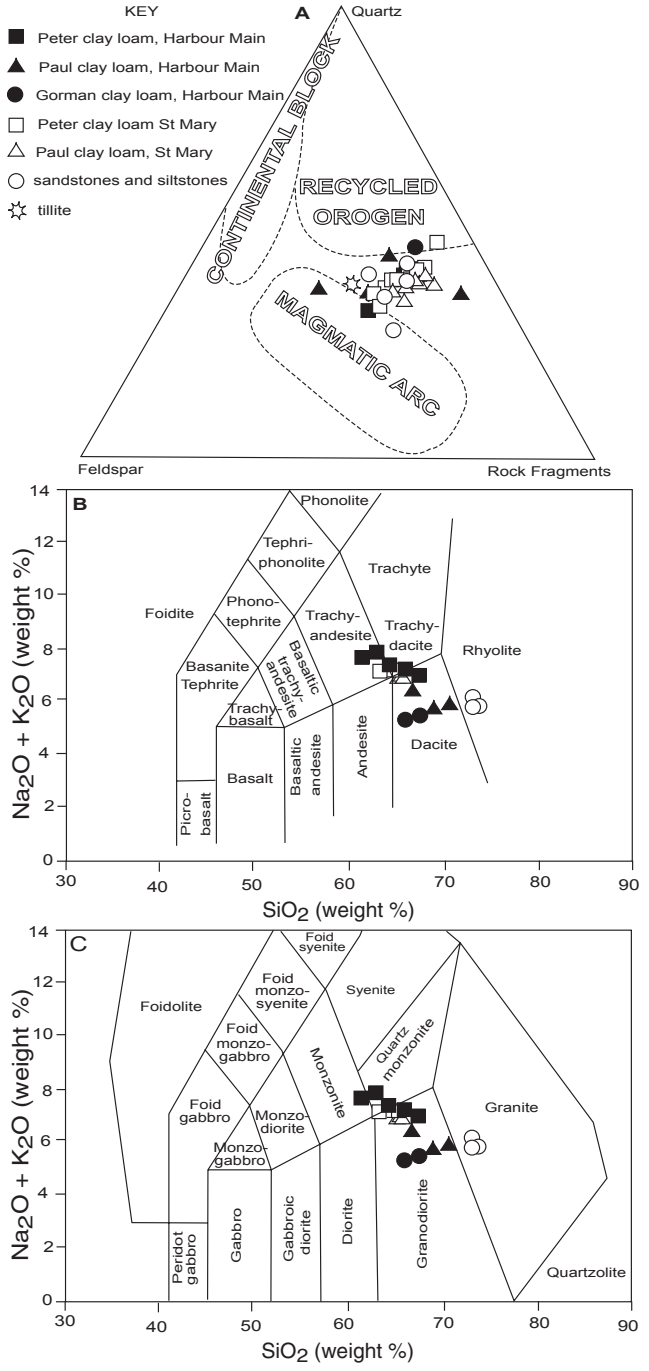

Fig. 11. Petrographic (**a**) and chemical (**b**, **c**) composition of analysed rocks from the Gaskiers Formation, in schemes of (**a**) Dickinson & Suczek (1979), (**b**) Le Bas *et al*. (1986) and (**c**) Middlemost (1994).

Unlike Miocene California, however, the Gaskiers Formation formed in a forearc basin of an active andesitic and rhyolitic volcanic arc, now represented by volcanic rocks of the same geological age near Marystown (O'Brien *et al*. 2001) and the islands of St. Pierre and Miquelon (Rabu *et al*. 1993). Thus a more appropriate analogue may be the Eocene–Oligocene marine Eugene Formation and non-marine Fisher Formation of the southern Willamette Valley, which accumulated between a coastal ridge (Siletzia terrane) and the proto-Cascadian volcanic arc of Oregon (Wells *et al*. 1998). The 1546 m of Eugene Formation between a tuff dated at 40.98 ± 0.56 Ma and another dated at 25.87 ± 0.59 Ma (Retallack *et al*. 2004) gives a rock accumulation rate of 0.10 ± 0.007 mm a^{-1}, and a precompaction (assuming 1 km overburden) sediment accumulation rate of 0.13 ± 0.009 mm a^{-1} (error includes standard error of linear regression between these and six other high-precision radiometric dates). These rates are the same order of magnitude as for the Gaskiers Formation and Conception Group.

My own observations of the upper Mall Bay Formation, especially that part of the formation above a prominent angular discordance (Eyles & Eyles 1989), do not support a deep marine turbidite interpretation. Much of the Mall Bay Formation measured for this study (Fig. 5) is sandy facies: massive to trough cross-bedded sandstone, with grey claystone breccia along basal scours. The rest of the uppermost Mall Bay Formation is a siltstone–shale facies with ripple marks, lenticular beds, shale flasers, soft sediment slumps, and sandy beds that have sharp tops as well as bottoms (Fig. 4d and e). These last deposits are more like tempestites (storm deposits) than turbidites (Seilacher 1982). The sandy facies is similar to estuarine palaeochannels and the siltstone–shale facies is like intertidal facies, especially those of the modern North Sea coast of Germany (Reineck & Singh 1973). By this interpretation of the uppermost Mall Bay Formation, sea level was retreating before the main glaciation represented by tillites of the Gaskiers Formation, and sea level rose within comparable intertidal facies of the basal Drook Formation.

Palaeosols of the Gaskiers Formation are chemically oxidized (Fig. 8) and show soil structures including cracking (Fig. 6a and b) and sand crystals (Fig. 7d and e), which are evidence for soil formation above water table (Dan & Yaalon 1982; Vepraskas & Sprecher 1997). The massive tillite above the palaeosols studied at St. Mary is 11 m thick, and entirely red and oxidized. This and other tillites contain large slightly deformed blocks of sediment (Eyles & Eyles 1989) including blocks of dolomicrite at all angles to bedding (Fig. 6c). These are all features of a ground moraine with local relief of at least 11 m, and a coastal glacier picking up blocks of frozen lacustrine dolomicrite and fluvial sandstone, as well as clay and river pebbles, like glacial moraines of coastal southwestern New Zealand (Tovar *et al*. 2008). Marine tillites in contrast have bedding, and lack solifluction blocks, as demonstrated by recent deposits in fiords of Svalbard (Ingolfsson 2011) and Ediacaran diamictites of the Poudingue de Granville on the Normandy coast of France (Eyles 1990; Retallack 2012*a*).

A non-marine depositional setting followed by weathering within a ground moraine also explains geochemical features of the Gaskiers Formation. C/S ratios in the Gaskiers Formation range from marine (0.001) to freshwater (30) values (Figs 2 and 3). Modern C/S values greater than 9.6 are freshwater (<1‰ salinity), as calibrated by C/S and salinity measurements in Chesapeake Bay, USA (Berner & Raiswell 1984). Quaternary marine C/S ratios average 2.8, whereas Tertiary–Devonian marine C/S ratios average 1.8 ± 0.5, and Cambrian–Ordovician marine C/S ratios average 0.5 ± 0.1; perhaps because of terrestrial ecosystems less productive of refractory organic matter before the Devonian (Raiswell & Berner 1986). The C/S ratio discriminating marine from nonmarine Ediacaran sediments is not known, although it is potentially determinable with additional studies like this one in which freshwater and marine values alternate, but a value of less than 9.6 was used here, and more of the samples than shown in Figures 2 and 3 were freshwater. Measured Fe_{HR}/Fe_{TOT} ratios are less than average Quaternary marine values (Ku *et al*. 2008), and some fall within the field of Quaternary soils (Fig. 2). These results are comparable with analyses reported here as evidence of palaeosol oxidation (Fig. 8; Table 2). Sulphur isotopic compositions in pyrite of the Gaskiers Formation are generally positive, as is typical for igneous and late diagenetic pyrite of little weathered clasts, rather than sulphate

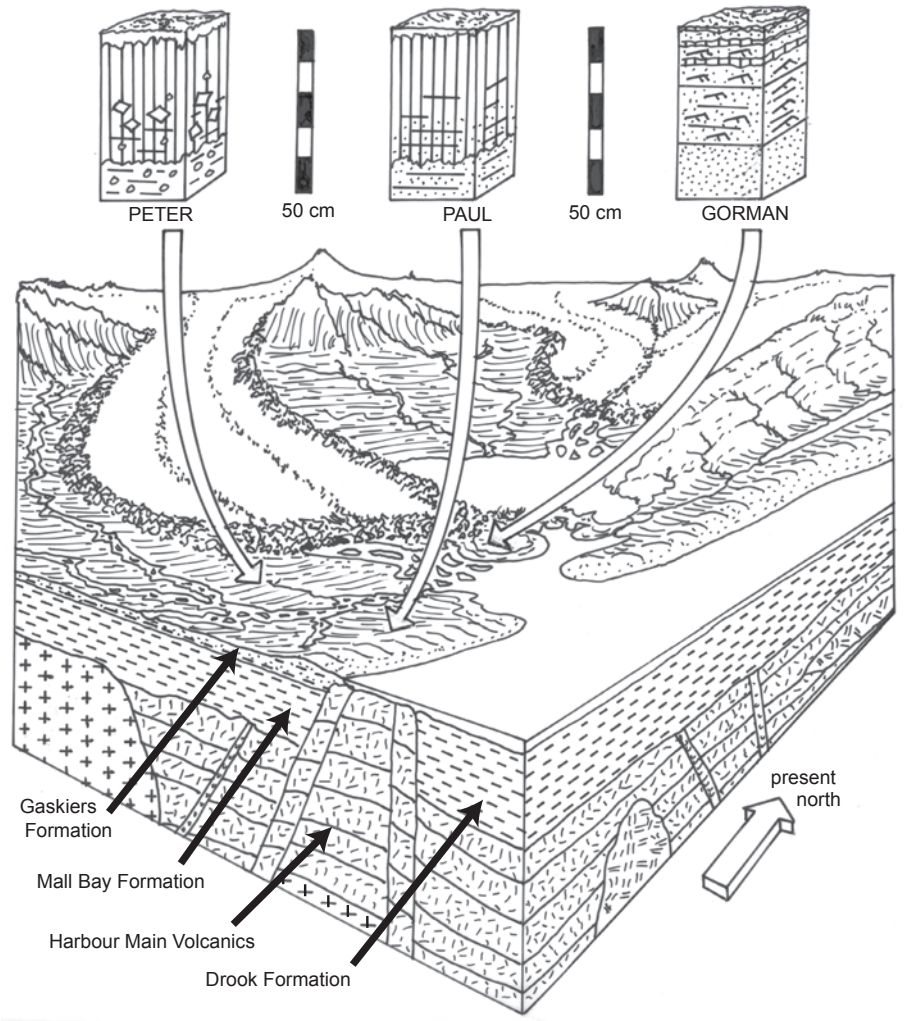

Fig. 12. Conjectural reconstruction of the sedimentary palaeoenvironment of the Gaskiers Formation in Newfoundland. Symbols as for Figure 8 but oxidized parts of palaeosols are indicated by vertical lines.

reduction in a euxinic marine basin (Canfield *et al*. 2007) or intertidal soils (Altschuler *et al*. 1983). Carbon and oxygen isotopic values from large dolomicrite clasts in the upper Gaskiers Formation near Harbour Main are both unusually depleted (Myrow & Kaufman 1999), as is typical for pedogenic carbonate (Knauth *et al*. 2003) or carbonate weathered by meteoric solutions (Knauth & Kennedy 2009). Very negative $\delta^{18}O_{PDB}$ values are indicative of marked Rayleigh fractionation from normal marine values; either inland or at high latitude or altitude (Knauth *et al*. 2003).

Palaeoclimate

Former temperature and precipitation can be inferred from chemical composition of palaeosols. The palaeohyetometer of Sheldon *et al*. (2002) uses chemical index of alteration without potash ($R = 100mAl_2O_3/(mAl_2O_3 + mCaO + mNa_2O)$, in moles), which increases with mean annual precipitation (P in mm) in modern soils ($R^2 = 0.72$; SE = ± 182 mm), as follows:

$$P = 221e^{0.0197R}. \quad (7)$$

This formulation is based on the hydrolysis equation of weathering, which enriches alumina at the expense of lime, magnesia, potash and soda. Magnesia is ignored because it is not significant for most sedimentary rocks, and potash is excluded because it can be enriched during deep burial alteration of sediments (Maynard 1992).

A useful palaeotemperature proxy for palaeosols devised by Sheldon *et al*. (2002) uses alkali index ($N = (K_2O + Na_2O)/Al_2O_3$ as a molar ratio), which is related to mean annual temperature (T in °C) in modern soils by the following equation ($R^2 = 0.37$; SE = ± 4.4 °C):

$$T = -18.5N + 17.3 \quad (8)$$

Only Peter pedotypes are appropriate for these proxies because they are comparable in development with modern soils on which the proxies are based (Sheldon *et al*. 2002), and these equations yield mean annual temperatures of 6.9 ± 4.4 °C and mean annual precipitation of 1016 ± 182 mm for the lower Gaskiers Formation at St. Mary, and comparable values of 6.1 ± 4.4 °C and 922 ± 182 mm for the upper Gaskiers Formation at Harbour Main. Paul pedotypes are of marginal development for the proxy of Sheldon *et al*. (2002), but yield comparable values: 6.9 ± 4.4 °C and 1069 ± 182 mm at St. Mary, and 6.3 ± 4.4 °C and 825 ± 182 mm at Harbour Main. These were humid temperate palaeoclimates, reinforcing comparison of the Gaskiers Formation with modern glacial outwash sequences of coastal western New Zealand (Tovar *et al*. 2008).

Also indicative of palaeoclimate are oversize sedimentary clasts, including the laminated dolomicrite boulders at Harbour Main (Fig. 6c; Myrow & Kaufman 1999) and 'sediment rafts' of gritty sandstone at St. Mary (Eyles & Eyles 1989). These oversize and moderately deformed clasts of redeposited sediment have been interpreted as solifluction debris: soft sediment transported in a frozen state (Eyles & Eyles 1989). Deformation of the forward edges of these boulders and small-scale deformation seen within the palaeosols (Fig. 9h) are similar to periglacial convolutions within modern soils (French 1996). These are indications of freeze–thaw within the climatic zone of discontinuous permafrost, as in the current spruce taiga belt of southern Canada (Davis 2001).

Biota

Molar depletion of phosphorus in the palaeosols of the Gaskiers Formation (Fig. 10) is evidence for at least microbial life on land. Experimental studies of modern soils have shown that only organic ligands can significantly weather phosphorus from apatite in soils (Neaman *et al*. 2005). Another indication of living microbes is molar depletion of alkali and alkaline earth oxides ($CaO + MgO + Na_2O + K_2O$) in the palaeosols, from carbonic acid produced by CO_2 of soil respiration (Retallack 1997). Organic carbon within palaeosols of the Gaskiers Formation is preserved at much lower levels than in their sedimentary parent materials and cover rocks, and is only slightly more abundant near the surface of the palaeosols than deeper in the profile (Fig. 8). This is a distribution of organic matter found in biologically active oxidized palaeosols that have undergone decomposition of organic matter during early burial (Retallack 1991).

Petrographic studies of Gaskiers Formation palaeosols revealed a variety of puzzling tubular features, including drab haloes around dark clayey tubules (Fig. 9g) like those of the Cambrian problematicum *Prasinema gracile* (Retallack 2011*b*). This problematic fossil is comparable in all respects except size with drab-haloed root traces in Phanerozoic palaeosols (*Radicites erraticus* Arafiev & Naugolnykh 1998). The drab halo is scaled to the width of the organic tubule, and is an early diagenetic post-burial alteration (Retallack 2011*b*). Also found were filaments with acutely pointed side-branches (Fig. 9c) like *Prasinema nodosum* (Retallack 2011*b*). The original organic filaments of *Prasinema* may have been bundles of sheathed cyanobacteria, like modern *Microcoleus vaginatus* (Garcia-Pichel & Wojciechowski 2009), or bundles of fungal hyphae, like the rhizomorphs of honey mushroom, *Armillaria mellea* (Mihail & Bruhn 2005), or rhizines like those of bruised lichen, *Toninia sedifolia* (Poelt & Baumgärtner 1964).

No large fossils were found in palaeosols of the Gaskiers Formation, and comparable modern organisms to the various filamentous structures are microscopic, like those as known today from biological soil crusts (Belnap & Lange 2003). In the terminology of Retallack (1992), these were microbial earths (Retallack 2012*b*). The pervasive destruction of bedding in palaeosols in the Gaskiers Formation is in part due to growth of evaporitic sand crystals (Fig. 7d and e), but near palaeosol surfaces was largely due to filamentous microbes.

Conclusions

The Gaskiers Formation was not what it has seemed: this study falsifies several previous interpretations of the Gaskiers Formation. It was not evidence of deep-sea anoxia as concluded by Canfield *et al*. (2007), because it included shallow marine and terrestrial facies (Fig. 5). It was not a deep marine till as proposed by Eyles & Eyles (1989), because palaeosols are evidence of terrestrial moraines (Fig. 8). It was not derived from a young oceanic island arc like the Antilles or Marianas as envisaged by Ichaso *et al*. (2007), but was deposited in a forearc basin from a complex arc with continental crust, like modern Japan (Fig. 12). Carbonate clasts in the uppermost part of the formation were considered unusual compared with cap carbonates reflecting extreme changes in global marine geochemistry by Myrow & Kaufman (1999), but here they are considered to be fragments of lacustrine dolomicrites altered by weathering (Fig. 6c). There is no evidence that the mid-latitude (34° ± 8°S; Pisarevsky *et al*. 2012) Gaskiers Glaciation extended into total sea ice cover and global carbon cycle perturbation as envisaged for 'Snowball Earth' glaciations of the Cryogenian (635–850 Ma; Hoffman *et al*. 1998; Hoffman & Schrag 2002). It was instead an unremarkable (non-'Snowball Earth') example of temperate glaciation of coastal mountains, like glaciers of modern New Zealand (Tovar *et al*. 2008).

The main reason for this radical reinterpretation is the discovery of palaeosols in the Gaskiers Formation. Palaeosols have long been known at Precambrian geological unconformities (Rye & Holland 1998), but have only recently been recognized in Precambrian sedimentary sequences (Retallack 2011*a*, *b*, 2012*a*, *b*). Precambrian palaeosols lack the obvious root traces and fossil stumps of Devonian and geologically younger palaeosols (Retallack 1997). Their gradational soil horizons beneath sharply truncated tops can be misinterpreted as graded beds (Retallack 2012*b*). Ediacaran palaeosols of the Gaskiers Formation show surficial enrichment of clay (Fig. 8) that is very distinct from the fine tail of clay settling from suspension after turbidite deposition (Retallack 2012*a*).

Soil structures in Ediacaran palaeosols can be misinterpreted as merely lack of bedding or as 'early diagenetic' features, but have distinctive characters of their own (Retallack 2011*a*, *b*). Clay-lined cracks defining irregular blocky units of palaeosol (Fig. 7b) are similar to cutans (argillans) defining soil clods (peds; Retallack 1997). Patches of highly birefringent clay in less birefringent matrix (Fig. 9d and e) are similar to sepic plasmic fabric of soils, produced under the uniquely local deviatoric stresses of weathering (Brewer 1976).

Especially diagnostic of Ediacaran palaeosols is geochemical differentiation characteristic of biologically active soils, including clay formation (Fig. 8), alkali and alkaline earth depletion, and pronounced depletion of P (Fig. 10; Neaman *et al*. 2005). Palaeosols show a diagnostic mass depletion of alkali and alkaline earths as well as volume loss compared with parent materials (Brimhall *et al*. 1992), whereas sedimentary graded beds show surface enrichment of alkali and alkaline earths and volume gain compared with parent materials (tidalite of Fig. 10). These indications of biologically promoted hydrolysis and nutrient acquisition in soils are supplemented by a variety of filamentous bedding disruptions as evidence for Ediacaran life on land (Fig. 9c and g). Without permineralization or carbonaceous preservation in the highly oxidized palaeosols of the Gaskiers Formation, the biological affinities of this early terrestrial life remain unknown. Nevertheless, the distribution and petrographic appearance of these palaeosols are compatible with microbial earth ecosystems (Retallack 2012*b*), broadly similar to modern biological soil crusts (Belnap & Lange 2003).

Fieldwork was funded in part by the University of Oregon, and aided by D. Retallack. Thanks are due to N. Sheldon, G. Narbonne, D. Erwin, S. Tweedt, M. La Flamme and P. Hoffman for useful discussion.

References

Alibés, B., Rothwell, R.G., Canals, M., Weaver, P.P.E. & Alonso, B. 1999. Determination of sediment volumes, accumulation rates and turbidite emplacement frequencies on the Madeira Abyssal Plain, NE Atlantic: A correlation between seismic and borehole data. *Marine Geology*, **160**, 225–250.

ALTSCHULER, Z.S., SCHNEPFE, M.M., SILBER, C.C. & SIMON, F.O. 1983. Sulphur diagenesis in Everglades peat and the origin of pyrite in coal. *Science*, **221**, 221–227.

ANDERSON, M.M. & KING, A.F. 1981. Precambrian tillites of the Conception Group on the Avalon Peninsula, southeastern Newfoundland. *In*: HAMBREY, M.J. & HARLAND, W.B. (eds) *Earth's Pre-Pleistocene Glacial Record*. Cambridge University Press, Cambridge, 760–766.

ARAFIEV, M.P. & NAUGOLNYKH, S.V. 1998. Fossil roots from the upper Tatarian deposits in the basin of the Sukhona and Malaya Severnaya Dvina Rivers: Stratigraphy, taxonomy and orientation paleoecology. *Paleontological Journal*, **32**, 82–96.

BAHLBURG, H. & DOBRZINKSI, N. 2011. A review of the chemical index of alteration (CIA) and its application to the Neoproterozoic palaeolatitudes and climate transitions. *In*: ARNAUD, E., HALVERSON, G.P. & SHIELDS-ZHOU, G. (eds) *The Geological Record of Neoproterozoic Glaciations*. Geological Society, London, Memoirs, **36**, 81–92.

BELNAP, J. & LANGE, O.L. (eds). 2003. *Biological Soil Crusts: Structure, Function and Management*. Springer, Berlin.

BERNER, R.A. & RAISWELL, R. 1984. C/S method for distinguishing freshwater from marine rocks. *Geology*, **12**, 365–368.

BOCKHEIM, J.G. 1990. Soil development rates in the Transantarctic Mountains. *Geoderma*, **47**, 59–77.

BOWRING, S.A., MYROW, P., LANDING, E. & RAMENZANI, J. 2003. Geochronological constraints on terminal Neoproterozoic events and the rise of metazoans. *National Astrobiology Institute General Meeting Abstracts*, **13045**, 113–114.

BREWER, R. 1976. *Fabric and Mineral Analysis of Soils*. Krieger, New York.

BRIMHALL, G.H., CHADWICK, O.A., *ET AL*. 1992. Deformational mass transport and invasive processes in soil evolution. *Science*, **255**, 695–702.

BROOKS, H.K. 1955. Clastic casts of halite crystal imprints from the Rome Formation (Cambrian) of Tennessee. *Journal of Sedimentary Petrology*, **25**, 67–71.

BRÜCKNER, R.D. & ANDERSON, M. 1971. Late Precambrian glacial deposits of southeastern Newfoundland—a preliminary note. *Geological Association of Canada Proceedings*, **24**, 95–102.

BUURMAN, P., JONGMANS, A.G. & PIPUJOL, M.D. 1998. Clay illuviation and mechanical clay infiltration: Is there a difference? *Quaternary International*, **51–52**, 66–69.

CANFIELD, D.E. & FARQUHAR, J. 2009. Animal evolution, bioturbation and the sulfate concentration of the oceans. *US National Academy of Sciences Proceedings*, **1106**, 8123–8127.

CANFIELD, D.E., POULTON, S.W. & NARBONNE, G.M. 2007. Late Neoproterozoic deep-ocean oxygenation and the rise of animal life. *Science*, **315**, 92–95.

CANFIELD, D.E., FARQUHAR, J. & ZERKLE, A.L. 2010. High isotope fractionations during sulfate reduction in a low-sulfate euxinic ocean analog. *Geology*, **38**, 415–418.

CARTO, S.L. & EYLES, N. 2011. The deep-marine glaciogenic Gaskiers Formation. Newfoundland, Canada. *In*: ARNAUD, E., HALVERSON, G.P. & SHIELDS-ZHOU, G. (eds) *The Geological Record of Neoproterozoic Glaciations*. Geological Society, London, Memoirs, **36**, 467–473.

CROWELL, J. (ed). 2003. Evolution of the Ridge Basin, Southern California: An Interplay of Sedimentation and Tectonics. Geological Society of America, Special Papers, **367**.

DAN, J. & YAALON, D.H. 1982. Automorphic saline soils in Israel. *In*: YAALON, D.H. (ed.) *Aridic Soils and Geomorphic Processes*. *Catena Supplement*, 103–115.

DAN, J., MOSHE, R. & ALPEROVICH, N. 1973. The soils of Sede Zin. *Israel Journal of Earth Sciences*, **22**, 211–227.

DAVIS, N. 2001. *Permafrost: A Guide to Frozen Ground in Transition*. University of Alaska Press, Fairbanks.

DICKINSON, W.R. & SUCZEK, C.A. 1979. Plate tectonics and sandstone composition. *AAPG Bulletin*, **63**, 2164–2182.

EVANS, D.A.D. & RAUB, T.D. 2011. Neoproterozoic palaeolatitudes: A global update. *In*: ARNAUD, E., HALVERSON, G.P. & SHIELDS-ZHOU, G. (eds) *The Geological Record of Neoproterozoic Glaciations*. Geological Society, London, Memoirs, **36**, 93–112.

EWING, S.A., SUTTER, B., *ET AL*. 2006. A threshold in soil formation at Earth's arid–hyperarid transition. *Geochimica et Cosmochimica Acta*, **70**, 5291–5322.

EYLES, N. 1990. Marine debris flows: Late Precambrian 'tillites' of the Avalonian–Cadomian Orogenic Belt. *Palaeogeography, Palaeoclimatology, Paleoecology*, **79**, 73–98.

EYLES, C.H. & EYLES, N. 1989. Glacially influenced deep marine sedimentation of the late Precambrian Gaskiers Formation, Newfoundland, Canada. *Sedimentology*, **36**, 601–620.

FOOD AND AGRICULTURE ORGANIZATION 1974. *Soil Map of the World. Vol I, Legend*. United Nations Educational Scientific and Cultural Organization, Paris.

FRENCH, H.M. 1996. *The Periglacial Environment*. Longman, Harlow.

GARCIA-PICHEL, F. & WOJCIECHOWSKI, M.F. 2009. The evolution of a capacity to build supra-cellular ropes enabled filamentous cyanobacteria to colonize highly erodible substrates. *PloS One*, **4**, e7801-1-6.

GARDINER, S. & HISCOTT, R.N. 1988. Deep water facies and depositional setting of the lower Conception Group (Hadrynian), southern Avalon Peninsula. *Canadian Journal of Earth Sciences*, **25**, 1579–1594.

GILE, L.H., HAWLEY, J.W. & GROSSMAN, R.B. 1981. *Soils and Geomorphology in the Basin and Range Area of Southern New Mexico—Guidebook to the Desert Project*. New Mexico Bureau of Mines and Mineral Resources Memoir, **39**.

GONZÀLEZ-ÀLVAREZ, I. & KERRICH, R. 2012. Weathering intensity in the Mesoproterozoic and modern large-river systems: A comparative study in the Belt–Purcell Supergroup, Canada and USA. *Precambrian Research*, **208–211**, 174–196.

GRAVENOR, C.P. 1980. Heavy minerals and sedimentological studies in the glaciogenic Late Precambrian Gaskiers Formation of Newfoundland. *Canadian Journal of Earth Sciences*, **17**, 1331–1341.

GRAVENOR, C.P., STUPAVSKY, M. & SYMONS, D.T.A. 1982. Paleomagnetic characteristics of the Late Precambrian Gaskiers tillite of Newfoundland. *EOS Transactions American Geophysical Union*, **63**, 616.

HARDEN, J.W. 1982. A quantitative index of soil development from field descriptions: examples from a chronosequence in central California. *Geoderma*, **28**, 1–28.

HOFFMAN, P.F. & LI, Z.-X. 2009. A paleogeographic context for Neoproterozoic glaciation. *Palaeogeography Palaeoclimatology Palaeoecology*, **277**, 158–172.

HOFFMAN, P.F. & SCHRAG, D.P. 2002. The snowball Earth hypothesis: Testing the limits of global change. *Terra Nova*, **14**, 129–155.

HOFFMAN, P.F., KAUFMAN, A.J., HALVERSON, G.P. & SCHRAG, D.P. 1998. A Neoproterozoic snowball Earth. *Science*, **281**, 1342–1346.

ICHASO, A.A., DALRYMPLE, R.W. & NARBONNE, G.M. 2007. Paleoenvironmental and basin analysis of the late Neoproterozoic (Ediacaran) upper Conception and St. John's Groups, west Conception Bay, Newfoundland. *Canadian Journal of Earth Sciences*, **44**, 25–41.

INGOLFSSON, O. 2011. Fingerprints of Quaternary glaciations on Svalbard. *In*: MARTINI, I.P., FRENCH, H.M. & ALBERTI, A.P. (eds) *Ice-marginal and Periglacial Processes and Sediments*. Geological Society, London, Special Publications, **354**, 15–31.

ISBELL, R.F. 1996. *The Australian Soil Classification*. Commonwealth Scientific and industrial Research Organization, Melbourne.

KING, A.F. 1988. *Geology of the Avalon peninsula, Newfoundland*. Newfoundland Department of Mines Map, **88-01**.

KNAUTH, L.P. & KENNEDY, M.J. 2009. The late Precambrian greening of the Earth. *Nature*, **460**, 728–732.

KNAUTH, L.P., BRILLI, M. & KLONOWSKI, S. 2003. Isotope geochemistry of caliche developed on basalt. *Geochimica et Cosmochimica Acta*, **67**, 185–195.

KU, T.C.W., KAY, J., BROWNE, E., MARTINI, A.M., PETERS, S.C. & CHEN, M.D. 2008. Pyritization of iron in tropical coastal sediments: Implications for the development of iron, sulphur, and carbon diagenetic properties, Saint Lucia, Lesser Antilles. *Marine Geology*, **249**, 184–205.

LANDING, E. 1996. Avalon: Insular continent by the latest Precambrian. *In*: NANCE, R.D. & THOMPSON, M.D. (eds) *Avalonian and Related Peri-Gondwnan Terranes of the Circum-North Atlantic*. Geological Society of America, Special Papers, **304**, 29–63.

LE BAS, M.J., LE MAITRE, R.W., STRECKEISEN, A. & ZANETTIN, B. 1986. A chemical classification of volcanic rocks based on the total alkali–silica diagram. *Journal of Petrology*, **27**, 745–750.

LEBRON, I., HERRERO, J. & ROBINSON, D.A. 2009. Determination of gypsum content in dryland soils exploiting the gypsum–bassanite phase change. *Soil Science Society of America Journal*, **73**, 403–411.

LITTLE, M.G. & LEE, C.A. 2006. On the formation of an inverted weathering profile on Mount Kilimanjaro, Tanzania: Buried paleosol or groundwater weathering? *Chemical Geology*, **235**, 205–221.

MAYNARD, J.B. 1992. Chemistry of modern soils as a guide to interpreting Precambrian paleosols. *Journal of Geology*, **100**, 279–289.

MCNAMARA, A.K., NIOCAILL, C.M., VAN DER PLUIJM, B.A. & VAN DER VOO, R. 2001. West African proximity of the Avalon terrane in the latest Precambrian. *Geological Society of America Bulletin*, **113**, 1161–1190.

MIDDLEMOST, A.K. 1994. Naming materials in the magma/igneous rock system. *Earth-Science Reviews*, **37**, 215–224.

MIHAIL, J.D. & BRUHN, J.N. 2005. Foraging behaviour of *Armillaria* rhizomorph systems. *Mycological Research*, **109**, 1195–1207.

MURPHY, C.P. 1983. Point counting pores and illuvial clay in thin section. *Geoderma*, **31**, 133–150.

MYROW, P.M. & KAUFMAN, A.J. 1999. A newly discovered cap carbonate above Varanger age glacial deposits in Newfoundland. *Journal of Sedimentary Petrology*, **69**, 784–793.

NANCE, R.D., MURPHY, J.B. & KEPPIE, J.D. 2002. A Cordilleran model for the evolution of Avalonia. *Tectonophysics*, **352**, 11–31.

Narbonne, G., Dalrymple, R.W., La Flamme, M., Gehling, J. & Boyce, W.D. 2005. *Life after Snowball: Mistaken Point biota and the Cambrian of Avalon. Field Trip Guidebook.* North American Paleontological Convention, Halifax, Nova Scotia.

Neaman, A., Chorover, J. & Brantley, S.L. 2005. Implications of the evolution of organic acid moieties for basalt weathering over geological time. *American Journal of Science*, **305**, 147–185.

Nesbitt, H.W. & Young, G.M. 1982. Early Proterozoic climates and plate motions inferred from major element content of lutites. *Nature*, **299**, 715–717.

Nordstrom, D.K. 2003. Modeling low-temperature geochemical processes. *In*: Drever, J.L. (ed.) *Surface and Ground Water, Weathering and Soils, Vol. 5, Treatise on Geochemistry*. Elsevier–Pergamon, Oxford, 37–72.

O'Brien, S.J., Dunning, G.R., Dube, B., O'Driscoll, C.F., Sparkes, B., Israel, S. & Ketchum, J. 2001. New insights into the Neoproterozoic geology of the central Avalon Peninsula (parts of NTS map areas 1N/6, 1N/7 and 1N/3), eastern Newfoundland. *Newfoundland and Labrador Geological Survey Report*, **21**, 169–189.

Papezik, V.S. 1974. Prehnite–pumpellyite facies metamorphism of late Precambrian rocks of the Avalon Peninsula. *Canadian Mineralogist*, **12**, 463–468.

Passchier, S. & Erukanure, E. 2010. Palaeoenvironments and weathering regime of the Neoproterozoic Squantum 'Tillite', Boston Basin; no evidence of a snowball Earth. *Sedimentology*, **57**, 1526–1544.

Passchier, S. & Krissek, L.A. 2008. Oligocene–Miocene Antarctic continental weathering record and paleoclimatic implications, Cape Roberts Drilling project, Ross Sea, Antarctica. *Palaeogeography, Palaeoclimatology, Palaeoecology*, **260**, 30–40.

Pisarevsky, S.A., McCausland, P.J.A., Hodych, J.P., O'Brien, S.J., Tait, J.A. & Murphy, J.B. 2012. Paleomagnetic study of the late Neoproterozic Bull Arm and Crown Hill Formations (Musgravetown Group) of eastern Newfoundland: implications for Avalonia and West Gondwana paleogeography. *Canadian Journal of Earth Sciences*, **49**, 308–327.

Poelt, J. & Baumgärtner, H. 1964. Über Rhizinenstränge bei placodialen Flechten. *Österreich Botanische Zeitschrift*, **111**, 1–18.

Rabu, D., Guerrot, C., Doig, R., Tegyey, M., Murphy, J.B. & Keppie, J.D. 1993. Premières données géochronologiques sur Saint-Pierre-et-Miquelon. *Comptes Rendus de l'Académie des Sciences*, Série 2, **317**, 639–646.

Raiswell, R. & Berner, R.A. 1986. Pyrite and organic matter in Phanerozoic normal marine shales. *Geochimica et Cosmochimica Acta*, **50**, 1967–1976.

Reineck, H.-E. & Singh, I.B. 1973. *Depositional Sedimentary Environments, with Reference to Terrigenous Clastics*. Springer, Berlin.

Retallack, G.J. 1991. Untangling the effects of burial alteration and ancient soil formation. *Annual Review of Earth and Planetary Sciences*, **19**, 183–206.

Retallack, G.J. 1992. What to call early plant formations on land. *Palaios*, **7**, 508–520.

Retallack, G.J. 1997. *A Colour Guide to Palaeosols*. Wiley, Chichester.

Retallack, G.J. 2005. Pedogenic carbonate proxies for amount and seasonality of precipitation in paleosols. *Geology*, **33**, 333–336.

Retallack, G.J. 2011*a*. Neoproterozoic glacial loess and limits to snowball Earth. *Journal of the Geological Society, London*, **168**, 1–19.

Retallack, G.J. 2011*b*. Problematic megafossils in Cambrian palaeosols of South Australia. *Palaeontology*, **54**, 1223–1242.

Retallack, G.J. 2012*a*. Were Ediacaran siliciclastics of South Australia coastal or deep marine? *Sedimentology*, **59**, 1208–1236.

Retallack, G.J. 2012*b*. Criteria for distinguishing microbial mats and earths. *In*: Noffke, N. & Chafetz, H. (eds) *Microbial Mats in Siliciclastic Sediments*. Society of Economic Paleontologists and Mineralogists, Special Papers, **101**, 136–152.

Retallack, G.J. & Huang, C.-M. 2010. Depth to gypsic horizon as a proxy for paleoprecipitation in paleosols of sedimentary environments. *Geology*, **38**, 403–406.

Retallack, G.J. & Jahren, A.H. 2008. Methane release from igneous intrusion of coal during Late Permian extinction events. *Journal of Geology*, **116**, 1–20.

Retallack, G.J., Krull, E.S. & Bockheim, J.G. 2001. New grounds for reassessing palaeoclimate of the Sirius Group, Antarctica. *Journal of the Geological Society, London*, **158**, 925–635.

Retallack, G.J., Orr, W.N., Prothero, D.R., Duncan, R.A., Kester, P.R. & Ambers, C.P. 2004. Eocene–Oligocene extinction and paleoclimatic change near Eugene, Oregon. *Geological Society of America Bulletin*, **116**, 817–839.

Rieu, R., Allen, P.A., Plötze, M. & Pettke, T. 2007. Compositional and mineralogical variations in a Neoproterozoic glacially influenced succession, Mirbat area, southern Oman: Implications for palaeoweathering conditions. *Precambrian Research*, **154**, 248–265.

Rye, R. & Holland, H.D. 1998. Paleosols and the evolution of atmospheric oxygen: a critical review. *American Journal of Science*, **298**, 621–672.

Seilacher, A. 1982. Distinctive features of sandy tempestites. *In*: Einsele, G. & Seilacher, A. (eds) *Cyclic and Event Stratification*. Springer, Berlin, 333–349.

Sheldon, N.D. & Retallack, G.J. 2001. Equation for compaction of paleosols due to burial. *Geology*, **29**, 247–250.

Sheldon, N.D., Retallack, G.J. & Tanaka, S. 2002. Geochemical climofunctions from North American soils and application to paleosols across the Eocene–Oligocene boundary in Oregon. *Journal of Geology*, **110**, 687–696.

Soil Survey Staff. 2010. *Keys to Soil Taxonomy*. USDA Natural Resources Conservation Service, Washington, DC.

Terry, R.D. & Chilingar, G.V. 1955. Summary of 'Concerning some additional aids in studying sedimentary formations,' by M. S. Shvetsov. *Journal of Sedimentary Petrology*, **25**, 229–234.

Thompson, M.D., Barr, S.M. & Grunow, A.M. 2012. Avalonian perspectives on Neoproterozoic paleogeography: evidence from Sm–Nd isotope geochemistry and detrital zircon geochronology in SE New England. USA. *Geological Society of America Bulletin*, **124**, 517–531.

Tominaga, M., Lyle, M. & Mitchell, N.C. 2011. Seismic interpretation of pelagic sedimentation in the 18–53 Ma eastern equatorial Pacific: Basin-scale sedimentation and infilling of abyssal valleys. *Geochemistry, Geophysics, Geosystems*, **12**, Q03004, doi:10.1029/2010GC003347.

Tovar, D.S., Shulmeister, J. & Davies, T.R. 2008. Evidence for a landslide origin of New Zealand's Waiho Loop moraine. *Nature Geoscience*, **1**, 524–526.

Ufnar, D.F., Gröcke, D.R. & Beddows, P.A. 2008. Assessing pedogenic calcite stable-isotope values: can positive linear covariant trends be used to quantify paleo-evaporation rates? *Chemical Geology*, **356**, 45–51.

Vepraskas, M.J. & Sprecher, S.W. 1997. Summary. *In*: Vepraskas, M.J. & Sprecher, S.W. (eds) *Aquic Conditions and Hydric Soils: The Problem Soils*. Soil Science Society of America, Special Publications, **150**, 153–156.

Wells, R.E., Weaver, C.S. & Blakely, R.J. 1998. Fore-arc migration in Cascadia and its neotectonic significance. *Geology*, **26**, 759–762.

Williams, H. & King, A.F. 1979. *Trepassey Area, Newfoundland*. *Geological Survey of Canada Memoir*, **389**.

Wood, D.A., Dalrymple, R.W., Narbonne, G.M., Gehling, J.G. & Clapham, M.E. 2003. Paleoenvironmental analysis of the late Neoproterozoic Mistaken Point and Trepassey Formations, southeastern Newfoundland. *Canadian Journal of Earth Sciences*, **40**, 1375–1391.

Yaalon, D.H., Moshe, R. & Nissim, S. 1982. Evolution of reg soils in southern Israel and Sinai. *Geoderma*, **28**, 173–202.

Ziegenbalg, S.B., Brunner, B., *et al.* 2010. Formation of secondary carbonates and native sulphur in sulphate-rich Messinian strata, Sicily. *Sedimentary Geology*, **227**, 37–50.

Received 19 April 2012; revised typescript accepted 20 August 2012.
Scientific editing by Philip Donoghue.